

University of Central Florida

STARS

Honors Undergraduate Theses

2024

Handheld X-ray Fluorescence (HHXRF) as a Non-Destructive Method for Trace Element Analysis of Ancient Maya (Pre-Conquest 800 BC - AD950) Teeth from Altun Ha, Belize

Griffon G. Binkowski

University of Central Florida, is299874@ucf.edu



Part of the [Archaeological Anthropology Commons](#), [Biological and Physical Anthropology Commons](#), and the [Other Anthropology Commons](#)

Find similar works at: <https://stars.library.ucf.edu/hut2024>

University of Central Florida Libraries <http://library.ucf.edu>

This Open Access is brought to you for free and open access by STARS. It has been accepted for inclusion in Honors Undergraduate Theses by an authorized administrator of STARS. For more information, please contact STARS@ucf.edu.

STARS Citation

Binkowski, Griffon G., "Handheld X-ray Fluorescence (HHXRF) as a Non-Destructive Method for Trace Element Analysis of Ancient Maya (Pre-Conquest 800 BC - AD950) Teeth from Altun Ha, Belize" (2024). *Honors Undergraduate Theses*. 20.

<https://stars.library.ucf.edu/hut2024/20>

HANDHELD X-RAY FLUORESCENCE (HHXRF) AS A NON-DESTRUCTIVE
METHOD FOR TRACE ELEMENT ANALYSIS OF ANCIENT MAYA (PRE-
CONQUEST 800 BC - AD 950) TEETH FROM ALTUN HA, BELIZE

by

GRIFFON BINKOWSKI

A thesis submitted in partial fulfillment of the requirements
for the Honors Undergraduate Thesis program in Anthropology
in the College of Science
and in the Burnett Honors College
at the University of Central Florida
Orlando, Florida

Spring 2024

Thesis Chair: Dr. Lana Williams

ABSTRACT

In anthropology, elemental analysis of bone and teeth can provide significant details about an individual's life history such as diet, toxicity exposure, residency, and migration patterns. Intra-individual comparisons can help to gather information about a single individual's life, while inter-individual comparisons can help illustrate a community's life history during these periods. However, current methods of elemental analysis commonly involve destruction of skeletal samples, which can damage a collection's integrity and be perceived as disrespectful by descendant communities. Preliminary research has validated handheld x-ray fluorescence spectrometry (HHXRF) as an accurate and reliable method of analysis appropriate for determining the elemental composition of archaeological bone and teeth. In this study, teeth from 16 individuals (N=16) from the pre-conquest Classic Period (AD 625-1100) Maya site of Altun Ha, Belize were analyzed using HHXRF to identify trace elements to gain a better understanding of the lives of the individuals and community. This study expands upon preliminary research by increasing the sample size and utilizes a filter to increase sensitivity to elements of interest. Diet and mobility were assessed using calcium (Ca), strontium (Sr), and bromine (Br) ratios. Net photon counts per element of interest were extracted and converted into ratios. An inter- and intra-individual comparison model was used. Results of calculated Sr/Ca ratios show a general increased reliance on marine subsistence sources within the sample. Shifts that do not align with this trend are present in several individuals, indicating social complexity of Altun Ha. Results of Br/Ca ratios are less clear in regard to diet and warrant further investigation.

ACKNOWLEDGMENTS

This study would not be possible without the people who have helped me throughout my life and undergraduate career.

There are not enough words to fully express my thanks to my thesis chair, Dr. Lana Williams. Thank you for the opportunity to conduct undergraduate research, for encouraging and nurturing my scientific curiosity, for your endless kindness and patience, and for your time and the opportunity to learn from your expertise. Thank you for allowing me the opportunity to work with human remains; it is truly a privilege. To the people to whom these remains belong, thank you for your story. Though we never met and never will, I feel honored to have gotten to know you better through what you left behind.

Thank you to Dr. Brigette Kovacevich for serving on my committee, for allowing me to use the HHXRF device, and for teaching me how to use the associated programs. This device has inspired me to explore more non-destructive ways to study past peoples. My sincere appreciation for your time, patience, expertise, and positivity cannot be understated.

Thank you to Dr. Sarah Freidline for assistance with the R programming and statistics used in this study. Thank you for providing your valuable time and expertise; I have developed a deep respect for R and statistics in anthropology because of your help.

I would also like to offer a huge ‘thank you’ to my loving family and amazing friends. Thank you to Melissa Marks, an incredibly talented anthropologist and caring friend. Thank you for quelling my midnight panic attacks and providing valuable insight on the statistics used in this study. To Mom, Dad, Natalie, and especially Grandma, although you do not know exactly what I am studying, I thank you for your constant support and encouragement. To Miranda and Chandler, thank you for being my best friends and supporting everything I do. I love you guys.

To my Education family at the Orange County Regional History Center, thank you for all that you do. Keep bringing our collective past to the public.

TABLE OF CONTENTS

LIST OF FIGURES	vi
LIST OF TABLES	ix
CHAPTER ONE: INTRODUCTION.....	1
Research Purpose	3
Ethical Considerations.....	3
CHAPTER 2: LITERATURE REVIEW	5
The Ancient Maya Diet: Lowlands and Coastal Locations.....	7
Intra- and Inter-Individual Comparisons.....	8
X-ray fluorescence spectrometry.....	8
Previous Studies Implying Diet, Health, Mobility, and Toxicity Exposure Using XRF	9
CHAPTER 3: MATERIALS AND METHODS	12
Site Description	12
Sample Selection	12
Data Collection Methods.....	17
Data Analysis	19
CHAPTER FOUR: RESULTS OF STUDY.....	20
Intra-individual Results	20
Intra-individual Spectral Assays.....	20

Inter-individual Results	22
Inter-individual Qualitative Assessment	22
Inter-individual Semi-Quantitative Statistics	28
CHAPTER FIVE: DISCUSSION OF RESULTS	29
Implying Diet and Mobility	29
Insights Gained from Strontium	29
Insights Gained from Bromine	30
Social Complexity in Altun Ha	32
Applications of HHXRF in Bioarcheology	33
CHAPTER SIX: CONCLUSIONS AND FUTURE RESEARCH.....	35
Study Limitations	36
Future Directions.....	37
APPENDIX A: HHXRF SPECTRA.....	38
APPENDIX B: NET PHOTON COUNTS	43
APPENDIX C: TRACE ELEMENT NET PHOTON COUNT RATIOS	48
APPENDIX D: TRACE ELEMENT NET PHOTON COUNT RATIO MEANS	53
REFERENCES	56

LIST OF FIGURES

Figure 1: Adapted map of relevant sites in Mesoamerica. Altun Ha is highlighted. (White et. al. 2001)	13
Figure 2: Culturally modified incisors of individual AH-E-44/2. (Image by Griffon Binkowski)	15
Figure 3: Bruker HHXRF positioned in acrylic stand (Image by Griffon Binkowski)	18
Figure 4: HHXRF spectra of M2 and I1 from individual AH-E-44/10. Br stands for bromine; Sr stands for strontium. Ca stands for calcium. M2 is represented by green, I1 is represented by blue.....	21
Figure 5: HHXRF spectra of M1, I1, and M3 from individual AH-K-29/8. Br stands for bromine; Sr stands for strontium. Ca stands for calcium. M1 is represented by gold, I1 is represented by blue, and M3 is represented by red.	21
Figure 6: Boxplots of sample Ca/P ratios organized by chronological formation of each tooth. .	23
Figure 7: Boxplots of sample Sr/Ca organized by chronological formation of each tooth	24
Figure 8: Boxplots of sample Br/Ca ratios organized by chronological formation of each tooth.	25
Figure 9: Strip chart of Sr/Ca ratio means of all individuals from the sample.	26
Figure 10: Strip chart of Br/Ca ratio means of all individuals from the sample.....	27
Figure 11: HHXRF spectra of I1 and M1 from individual AH-C-13/5 A. Br stands for bromine; Sr stands for strontium. Ca stands for calcium. M1 is represented by gold, I1 is represented by blue.....	27
Figure 12: HHXRF spectra of I1 and M1 from individual AH-C-13/5 D. Br stands for bromine; Sr stands for strontium. Ca stands for calcium. M1 is represented by gold, I1 is represented by blue, and M3 is represented by red.	28

Figure 13: HHXRF spectra of M2, I1, and M3 from individual AH-C-13/14. Br stands for bromine; Sr stands for strontium. Ca stands for calcium. M2 is represented by green, I1 is represented by blue, and M3 is represented by red. 29

Figure 14: HHXRF spectra of M2 and I1 from individual AH- C-13/20. Br stands for bromine; Sr stands for strontium. Ca stands for calcium. M2 is represented by green, I1 is represented by blue, and M3 is represented by red. 30

Figure 15: HHXRF spectra of M2, I1, and M3 from individual AH-C-13/33. Br stands for bromine; Sr stands for strontium. Ca stands for calcium. M2 is represented by green, I1 is represented by blue, and M3 is represented by red. 31

Figure 16: HHXRF spectra of M2, I1, and M3 from individual AH-E-44/2. Br stands for bromine; Sr stands for strontium. Ca stands for calcium. M2 is represented by green, I1 is represented by blue, and M3 is represented by red. 32

Figure 17: HHXRF spectra of M2 and I1 from individual AH-E-44/3. Br stands for bromine; Sr stands for strontium. Ca stands for calcium. M2 is represented by green, I1 is represented by blue. 33

Figure 18: HHXRF spectra of M2, I1, and M3 from individual AH-E-44/7. Br stands for bromine; Sr stands for strontium. Ca stands for calcium. M2 is represented by green, I1 is represented by blue, and M3 is represented by red. 34

Figure 19: HHXRF spectra of M2 and I1 from individual AH-E-44/8. Br stands for bromine; Sr stands for strontium. Ca stands for calcium. M2 is represented by green, I1 is represented by blue. 35

Figure 20: HHXRF spectra of M2 and I1 from individual AH-E-44/10. Br stands for bromine; Sr stands for strontium. Ca stands for calcium. M2 is represented by green, I1 is represented by blue..... 36

Figure 21: HHXRF spectra of M2, I1, and M3 from individual AH-K-29/6. Br stands for bromine; Sr stands for strontium. Ca stands for calcium. M2 is represented by green, I1 is represented by blue, and M3 is represented by red..... 37

Figure 22: HHXRF spectra of M1, I1, and M3 from individual AH-K-29/8. Br stands for bromine; Sr stands for strontium. Ca stands for calcium. M1 is represented by gold, I1 is represented by blue, and M3 is represented by red..... 38

Figure 23: HHXRF spectra of M1, I1, and M3 from individual AH-K-29/18. Br stands for bromine; Sr stands for strontium. Ca stands for calcium. I1 is represented by blue, and M3 is represented by red..... 39

Figure 24: HHXRF spectra of M1, I1, and M3 from individual AH-K-29/19 Br stands for bromine; Sr stands for strontium. Ca stands for calcium. M1 is represented by gold, I1 is represented by blue, and M3 is represented by red..... 40

Figure 25: HHXRF spectra of M1, I1, and M3 from individual AH-K-35/5. Br stands for bromine; Sr stands for strontium. Ca stands for calcium. M1 is represented by gold, I1 is represented by blue, and M3 is represented by red..... 41

Figure 26: HHXRF spectra of M2, I1, and M3 from individual AH-K-35/6. Br stands for bromine; Sr stands for strontium. Ca stands for calcium. M2 is represented by green, I1 is represented by blue, and M3 is represented by red..... 42

LIST OF TABLES

Table 1: Preliminary data displaying averages of keV intensities for Ca and P for each tooth sample and individual (Binkowski, 2023)	11
Table 2: Altun Ha individuals and selected samples. R, right; L, left; U, undetermined.....	16
Table 3: ANOVA and Tukey's test results for trace element ratios of interest. Significant p-values are bolded.....	28
Table 4: Net photon counts of each element per assay per sample.	44
Table 5: Net photon count ratios for each assay per sample. Bolded values were excluded from analysis.....	49

CHAPTER ONE: INTRODUCTION

Investigating diet and mobility of individuals and communities is a crucial aspect of archaeological research. An estimation of diet can reveal details about the mobility, socioeconomic status, and agricultural practices of a community or individual. Archaeological skeletal remains contain trace elements useful when reconstructing these life histories. Teeth are known to be one of the most useful skeletal assets for analysis of trace elements due to their mostly inorganic composition and resilience to diagenesis (Byrnes and Bush 2016; Forshaw 2016). However, current methods of elemental analysis commonly involve destruction of skeletal samples. This can damage a collection's integrity, preventing future research and destroying seldom preserved remains. Additionally, destruction of these samples can be perceived as disrespectful by descendant communities. More so than ever, the implications of sample destruction and their effect on archaeologist and descendant community relationships must be seriously considered.

Recently, handheld x-ray fluorescence (HHXRF) spectrometry has been established as an accurate and reliable method of analysis appropriate for determining the elemental composition of archaeological bone and teeth (Hunt and Speakman 2015; Zimmerman et al. 2015). Unlike other techniques used for analysis of archaeological samples, x-ray fluorescence (XRF) spectrometry is a non-destructive analysis technique. Archaeological materials, such as skeletal remains, are unique in the sense that they have been preserved, often unintentionally. A non-destructive analytical approach ensures such materials are left intact, subsequently maintaining the integrity of a collection. This is especially pertinent in cases of culturally altered skeletal

remains which can yield important information about a population and individual and could be further studied. Non-destructive analysis additionally ensures that materials deemed culturally sensitive by extant and descendant communities, such as skeletal remains, are treated in a respectful and ethical way. HHXRF offers a non-destructive alternative that can decrease tensions centered around skeletal remains destruction.

Comparatively, HHXRF spectrometry instruments are rapid, portable, and relatively simple to operate. These elements can be beneficial during fieldwork operations, where the most information might be gleaned from *in situ* analysis. Additionally, this can allow for students and professionals to be efficiently trained in how to use these devices. Therefore, further developments of HHXRF standards within bioarchaeology and additional verification of HHXRF's analytical abilities would be highly useful in situations where time, sample scarcity, and collection integrity are of great concern.

Intra-individual assessments of skeletal material can provide detailed insights into a single person's past. One common way to observe this is through dental remains, as each tooth develops during a specific period during an individual's life, resulting in mineralized trace elements during these specific periods (White et al. 2012). Although intra-individual analysis has been carried out mainly in stable isotope studies, to date no known studies investigating intra-individual life histories using trace elements discerned by HHXRF have been published (Simpson et al. 2021). Intra-individual life histories are important when inferring broader trends of the community; an intra-individual approach can reveal social complexities that may be occluded when examining larger group trends alone.

Research Purpose

The primary focus of this study is to investigate the diet and mobility of archaeologically recovered individuals from Altun Ha, Belize over a period of childhood to adolescence. This study also aims to contribute to the larger scope of developing methodological protocols for trace element discernment in archaeological teeth using HHXRF. Two levels of investigation will be done. At the intra-individual level, teeth samples representing different developmental periods in a single individual's life will be compared. At the inter-individual level, implied diet and mobility profiles from individuals will be compared to discern any possible trends. While it would be valuable to create an HHXRF standard for calibration and direct comparison of trace element results obtained from skeletal materials in bioarcheological contexts, it is beyond the scope of this project and may be pursued in the future.

The following chapters present background information relevant to trace element analysis regarding diet and mobility, HHXRF spectrometry, and the results of the net photon count calculations of the individuals from Altun Ha, Belize. Chapter 2 provides a literature review discussing the physics of XRF spectrometry, trace elements found in dental remains pertinent to diet and mobility, and prior work utilizing HHXRF when implying diet and mobility. Chapter 3 includes descriptions of the archaeological site of Altun Ha, Belize, criteria for sample selection, sample details, and methods of data collection and analysis. Chapter 4 presents the results of this study, and Chapter 5 discusses their methodological and contextual significance. Finally, Chapter 6 presents conclusions, limitations, and future considerations for this study.

Ethical Considerations

Human remains are essential to developing an understanding our collective past. However, procurement and analysis of human remains carry an ethical caveat. More now than

ever, discussion of inclusion, diversity, and respectful practices has entered anthropological discourses (Licata et al. 2020). The discipline of anthropology has a long history of disregarding human remains as the remnants of a past person, instead approaching handling, procurement, and analysis of remains with little regard to the deceased individual's humanity or the descendant community's wishes or beliefs (Licata et al. 2020). Many of the individuals and communities who hold, or should hold, stewardship of these archaeological remains have lost their autonomy and ability to consent to analysis. This study considers this power imbalance and history of irresponsible treatment of skeletal material, following a quote by Licata et al. (2020):

“These remains, even if dated hundreds or thousands of years ago, maintain their human dignity and force the community to reflect on the ethical issues related to their analysis, curation and display.”

It is essential that anthropologists follow ethical guidelines and principles of professional responsibility, such as those proposed by the American Anthropological Association (AAA) (2012). Remains of individuals were handled under supervision in an ethical manner and subjected to non-destructive analytical techniques. The individuals in this study are part of a collection maintained for the purpose of academic research and are not used for teaching purposes. The collection is curated with permission from the Institute of Archaeology (NICH) Belize, which is periodically revisited under the aegis of the Institute's Director and regional Indigenous descendent communities. In these ways, this study worked to act as ethically as possible during the data collection, analysis and reporting process.

CHAPTER 2: LITERATURE REVIEW

Trace Element Analysis in Biological Archaeology

In archaeological investigations into the lives of past individuals, trace element signatures in bone and tooth enamel can be employed as useful indicators of variables such as diet, mobility, health, and craft production. Trace elements calcium (Ca), nitrogen (N), zinc (Zn), and manganese (Mn), have been shown to provide information about diet and health (Pate 1994, Simpson et al. 2021). Heavy metals, like lead (Pb) and mercury (Hg), indicate toxicity exposure during daily activities (e.g., craft production) (Simpson et al. 2021). Information regarding diet and mobility can be gleaned from the trace element strontium (Sr) that has been incorporated into tooth enamel and bone. (Walton 2021, Schwartz 2021, Pate 1994, Simpson et al 2021). Recently, bromine (Br) has been proposed as an appropriate trace element for use in discerning marine from terrestrial diets (Martin et al. 2007, Dolphin et al. 2013). However, there is considerable debate around if Br is a good dietary indicator (Kozachuk et al. 2020). Information is gained from these trace elements by using elemental counts concentration ratios or elemental counts in parts per million (Schwartz 2021, Wright 2013, Wright et al. 2010).

Strontium has shown to be a preferential trace element when implying diet and mobility. This is due to several factors, including its relative quantities at different trophic levels and its propensity to be absorbed by the body when mineralizing Ca into skeletal elements (Pate 1994). Strontium is an alkaline earth metal found in abundance in soil and water. Plants absorb strontium and Ca through the soil and water. At this level, plants exhibit the highest level of concentration of Sr in the food web and are known to align with geologic elements of the local environment (Pate 1994). However, “Seeds and roots, discriminate against Ca in favor of Sr and thus have higher Sr/Ca ratios than the soil solution” (Pate 1994:166). When these plants are

eaten, a portion of the available strontium in the plants is absorbed by the consumer. Following this pattern, the amount of Sr decreases as trophic level increases (Pate, 1994). Pate (1994) notes that a diet high in terrestrial protein yields a low strontium concentration compared to the high strontium concentrations found in diets with heavy plant consumption. Additionally, a high Sr/Ca ratio in skeletal tissue is associated with marine foods. Due to the high Sr/Ca concentration found in saltwater, marine foods generally have greater Sr/Ca ratio in tissue than freshwater foods (Pate 1994). However, Pate (1994) notes that Sr/Ca values can sometimes overlap for marine and terrestrial sources, as many sediments also exhibit high Sr concentrations.

Bromine is an element found in high abundance in seawater (99%) and select marine organisms, with low quantities seen in the Earth's crust (Kozachuk et al. 2020). It is an essential element to the human body's function, and though research has linked the element to collagen formation, it has been noted that further investigation is warranted to fully explain bromine's role in the body (Kozachuk et al. 2020). Bromine enters the food web through direct growth in seawater or by a sea spray effect, where air containing sea water molecules "pollutes" plant growth in coastal areas (Wytttenbach et al. 1997). Bromine enters the body by direct consumption of marine organisms, consumption of organisms with a marine diet, or by consumption of sea spray contaminated organisms (Dolphin et al. 2013). Dolphin et al. (2013) noted that concentrations of Br varied in different modern and ancient populations, in which higher concentrations of bromine in tooth enamel, bone, and urine aligned with higher intake of foods of marine origin. Dolphin et al. (2013) also notes that some nuts also have a high Br concentration.

However, the hypothesis of Br as an appropriate dietary indicator was revisited in 2020, with Kozachuk et al. (2020) warning against using Br as a dietary indicator when marine diet is

not verified, noting low concentrations of Br in bony tissue and its affinity for organic portions of the bone. A study by Mariel et al. (2014) has shown Br at .01% concentrations in tooth enamel, which are consistently observed in the inner part of the enamel thickness. In comparison, Sr is observed at .09% in consistently low concentrations in the cusp tips and the inner part of the enamel thickness (Mariel et al. 2014). Martin et al. (2007) attributed widely dispersed bromine concentrations in bone in teeth to a marine diet in one pre-Colombian Peruvian sample. In general, the literature on bromine as a dietary indicator is limited and highly debated.

The Ancient Maya Diet: Lowlands and Coastal Locations

The diet of the ancient Maya is complex, being comprised of several components with notable staples. The ancient Maya derived food from agricultural implementations, hunting and gathering, and marine-estuary resources. Maize was the staple carbohydrate of the ancient Maya, occasionally supplemented by other wild plants and legumes. Maize production was intense and widespread, remaining at stable levels during the pre-classic period. During the Late Classic (AD 550-800) to Terminal Classic period (AD 800-950), maize production experienced a gradual decline. However, production experienced a stark increase through the post-Classic (AD 1000–1520) to Historic period (AD 1520-1670). Protein was derived from terrestrial and marine sources; deer and peccary are noted by faunal remains and isotopic data as a terrestrial source. Coastal locations frequently derived dietary items from the ocean and estuaries, such as fish, shellfish, and aquatic plant life. Reliance on maize is less so in coastal locations, though maize did remain a staple in these communities' diets (White 1989, White 2001). Among elites, maize was valued as a high-status food. At the coastal site of Altun Ha, there is evidence of Maya males consuming a higher amount of terrestrial meat when compared to females (White 2001).

Children of all regions, cultural groups, and environments began weaning during approximately the same age range of 3-4 years (White 2001).

Intra- and Inter-Individual Comparisons

When investigating diet and mobility, both intra- and inter-individual comparisons of trace element concentrations can be used to gain a better understanding of a community (Wright and Schwarcz 1998, Knudson et al. 2016, Koutamanis 2021). An inter-individual approach allows for generalized trends to be observed, while an intra-individual approach reveals a more detailed life history of a single individual. Combining these approaches allows researchers to observe a more detailed picture of the lives of individuals that otherwise may be occluded by a homogenized trend assessment. Utilizing teeth with differing periods of formation is a common and established method of observing potential changes in weaning, diet, and mobility in mammals (Wright and Schwarcz 1998, Knudson et al. 2016, Koutamanis 2021). means that the trace elements found within each tooth were incorporated during a distinct period in an individual's life, allowing for comparisons inter-tooth comparisons within an individual to reconstruct life history. These life histories can additionally be observed at the inter-individual level, revealing information about a group's collective life history.

X-ray Fluorescence Spectrometry

Both HHXRF instruments and benchtop XRF instruments are used to assay archaeological materials. Handheld XRF devices can be held directly to a sample and manually held in place while carrying out an assay. Alternatively, HHXRF devices can be positioned upright by way of a stand, allowing for use of a metal cover to cover the sample (Figure 1). Benchtop XRF instruments require samples to be placed into a vacuum sealed chamber, allowing

the XRF device to read lower atomic weight elements (Bonizzoni et al. 2013). Additionally, a vacuum attachment can be used with HHXRF devices to increase the range of elements that can be identified and amplify elements of a lighter atomic weight. X-ray fluorescence spectrometers work by bombarding a sample with x-rays. These incident x-rays destabilize the atoms in the sample, forcing electrons to be ejected from the orbital shell as a result. Electrons from outer orbits then move down into the inner orbits to stabilize the atom, emitting secondary fluorescent x-rays. Energy loss is determined by the distance an electron is from the nucleus. When an electron drops into a lower orbit, there is a subsequent loss of energy detected by XRF that correlates with specific elements present (Bruker, 2023).

Previous Studies Implying Diet, Health, Mobility, and Toxicity Exposure Using XRF

Multiple previous studies have been done utilizing XRF as a method of trace element analysis for use on modern primate and bioarcheological skeletal materials. In a preliminary study investigating the validity and accuracy of HHXRF when used to discern known calcium/phosphorous (Ca/P) ratios in skeletal material, Zimmerman et. al. (2015) utilized a Bruker Elemental S1 Turbo-SDR HHXRF with no filter for analysis. Samples consisting of human remains, nonhuman vertebrate remains, other biological materials, nonbiological materials, and materials modified taphonomically were assayed for 60 seconds of live time. Results indicated that “osseous and dental tissue can be distinguished from nonbone material of similar chemical composition” (Zimmerman et. al, 2015). Additionally, the HHXRF device used was shown to detect the atomically lighter element of phosphorous accurately and reliably without the use of a vacuum attachment.

Schwartz (2021) performed HHXRF analysis on bone and teeth samples representing six modern primates. A 90-second quantitative measurement and a 60-second qualitative

measurement was used with no added filter to assay the samples. Sr/Ca ratios yielded were within range for a known folivorous (leaf-eating) primate diets, verifying that HHXRF analysis and Sr/Ca ratios can be used to imply diet of primates.

Walton's (2021) elemental analysis of burials from Moho Cay, Belize included forty archaeological samples consisting of cortical bone, teeth, and one soil sample. A Bruker SD III tracer HHXRF device was used in addition to a 12 mil Al, 1 mil Ti, 6 mil Cu filter. Walton's findings yielded consistently high strontium levels when data from cortical bone and enamel assays were compared, aligning with the implied diet of marine resources of Moho Cay, Belize (Walton, 2021). Consistency in discerning levels of the trace element Sr between the two 120 live second assays for each sample showed accuracy and reliability of the methodology and device on skeletal remains in archaeological contexts like the site context of this study.

A preliminary investigation conducted prior to this study assessed the reliability and accuracy of the Bruker SD III tracer HHXRF device. Permanent teeth of four individuals from Altun Ha, Belize were sampled. Two 90 second assays without the use of a filter were performed on multiple planes on each tooth. Data yielded from peak intensities of calcium and phosphorous were ratioed, subsequently producing Ca/P ratios within the accepted range for archaeological tooth enamel (Zimmerman et. al. 2015; Quelch et. al.,1983). This preliminary investigation verifies HHXRF as an accurate and reliable method in which to identify trace elements within the materials from Altun Ha, Belize (Table 1).

Table 1: Preliminary data displaying averages of keV intensities for Ca and P for each tooth sample and individual (Binkowski, 2023)

Individual	<u>Incisor</u> Avg. keV (intensity)	<u>Molar</u> Avg. keV (intensity)	<u>3rd Molar</u> Avg. keV (intensity)	<u>TOTAL</u> Avg. keV (intensity)	<u>Mean Ca/P</u> <u>Ratio</u> (Based on averages)
AH-C-13/14	Ca: 3.6917±.09 P: 2.0137±.08	Ca: 3.6917±.09 P: 2.0137±.08	Ca: 3.6917±.09 P: 2.0137±.08	Ca: 3.6917±.09 P: 2.0137±.08	1.83
AH-C-13/20	Ca: 3.6917±.09 P: 2.0137±.08	Ca: 3.6917±.09 P: 2.0137±.08	-	Ca: 3.6917±.09 P: 2.0137±.08	1.83
AH-C-13/33	Ca: 3.6917±.09 P: 2.0137±.08	Ca: 3.6917±.09 P: 2.0137±.08	Ca: 3.6917±.09 P: 2.0137±.08	Ca: 3.6917±.09 P: 2.0137±.08	1.83
AH-E-44/2	Ca: 3.6917±.09 P: 2.0137±.08	Ca: 3.6917±.09 P: 2.0137±.08	Ca: 3.6917±.09 P: 2.0137±.08	Ca: 3.6917±.09 P: 2.0137±.08	1.83

Ca, calcium; P, phosphorus.

CHAPTER 3: MATERIALS AND METHODS

The Altun Ha skeletal materials are housed and curated in the Maya Archaeological Research Collections (MARC), which is in the UCF Department of Anthropology. Teeth from 16 adult individuals (N= 12 adult biological females and possible females, 3 adult biological males, 1 undetermined sex) from the site of Altun Ha, Belize were selected and analyzed. Ethical and research permissions are on record for this collection.

Site Description

Altun Ha is an ancient Maya city in the north-central coastal plain of Belize consisting of central and suburban zones occupied between 900 BC-AD 1000 (Figure 1). Materials in this study date from the Pre-classic Period (800 BC-AD 250), Late Classic (AD 550-800), and the Terminal Classic Period (AD 800-950). Over this time span, there was intensified maize production and a large marine/reef resources component in the diet as well as evidence for craft production, contact, and trade into western Mesoamerica. Individuals with the highest recognized status during Early Classic Period (AD 250-550) had the highest intake of maize. In the Late Classic (AD550-800), more maize was consumed in the central precinct than in the outer zones, with one outer zone having a higher degree of reef resources consumption than in other areas (White et al. 2001).

Sample Selection

The teeth selected for investigating diet and mobility were the central maxillary incisor (MI1), the first maxillary molar (MM1), the second maxillary molar (MM2), and the third



Figure 1: Adapted map of relevant sites in Mesoamerica. Altun Ha is highlighted. (White et. al. 2001)

maxillary molar (MM3). These teeth were selected based on their distinct periods of formation during childhood and adolescence. MM1 is the first adult tooth to form, with crown mineralization beginning at birth and completed by 2.5 – 4.5 years of age. MI1 is the second adult tooth to form, with crown mineralization beginning at 2.5-4 months after birth and completed at 4-5 years of age. MM2 crown mineralization begins at 2.5-3 years of age and is completed at 7-8 years of age. The final adult tooth to form is MM3; crown mineralization begins at 8-11 years of age and is completed by 12-15 years of age (White et al. 2012).

Mineralization of the crown ceases after these formation windows (White et al. 2012). This means the trace elements found within each tooth were incorporated during a distinct period in an individual's life, allowing for comparisons inter-tooth comparisons within an individual to reconstruct life history. Life histories can additionally be observed at the inter-individual level, revealing information about a group's collective life history. The canine and premolars were not considered in this study due to their inability to fully cover the HHXRF detection window.

The included individuals were selected based on their ability to produce samples best suited for HHXRF analysis. Although Byrnes and Bush (2016) recommend that the surface of osseous material be abraded to mitigate the effects of soil contamination, this defeats the non-destructive aspect of the present study. Each sample was visually inspected for possible contaminants such as soil or calculus. A total of 41 teeth exhibiting minimal contaminants were selected for analysis (Table 2). The second molar of individual AH-C-13/20 had a small formation of calculus that was removed with a dental tool and separately stored. Additionally, only samples exhibiting intact enamel with minimal wear were selected. Teeth with a high degree of enamel wear resulting in exposure of the dentin were excluded from this study. This was done to prevent the introduction of dentin into the detection beam when the primary target was crown enamel.

Several individuals in the collection exhibit dental modification such as filing, drilling, or added stone inlays (Figure 2). Filed tooth samples that did not greatly impact the degree of detection window coverage were included in this study. Eight individuals in the selected sample group exhibited dental modification (noted in Table 2).



Figure 2: Culturally modified incisors of individual AH-E-44/2. (Image by Griffon Binkowski)

Table 2: Altun Ha individuals and selected samples. R, right; L, left; U, undetermined.

Individual	Estimated Sex	Estimated Age	Teeth	Notes
AH-E-44/2	F	U	LMI1 LMM2 LMM3	Modified incisor
AH-E-44/8	U	Adult	RMI1 RMM2	Modified incisor
AH-E-44/7	M	Old	RMI1 RMM2	Modified incisor
AH-C-13/14	F	Adult	LMI1 LMM2 UMM3	Malformed 3rd molar, unable to side
AH-C-13/33	F	Old	RMI1 RMM2 RMM3	
AH-C-13/20	F	U	RMI1 RMM2	Calculus removed
AH-E-44/10	Possible F	U	LMI1 RMM2	Modified incisor
AH-E-44/3	M	Adult	LMI1 RMM2	Modified incisor
AH-K-29/8	F	Adult	LMI1 LMM1 LMM3	Modified incisor
AH-K-29/6	F	~20	LMI1 LMM2 RMM3	
AH-C-13/5 D	F	Old	RMI1 LMM1 LMM3	Modified incisor
AH-C-13/5 A	Possible F	Adult	RMI1 RMM1	Secondary internment burial.
AH-K-29/19	M	U	RMI1 LMM1 UMM3	Enamel malformation on 3rd molar, unable to side
AH-K-29/18	F	U	RMI1 RMM3	Original M1 reclassified as mandibular, omitted for consistency.
AH-K-35/5	F	U	LMI1 RMM1 LMM3	Modified incisor
AH-K-35/6	F	U	LMI1 RMM2 LMM3	Use wear pattern on 1st molar

Data Collection Methods

A Bruker Tracer III-SD handheld XRF spectrometer (HHXRF) was used to collect data on each sample. The parameters set for the HHXRF device for sample analysis was a tube setting of 40 KeV without the use of a vacuum, following the standards set by Walton (2021). Additionally, tube settings were adjusted to 25 μA instead of Walton's (2021) 12.70 μA , because a 90 second assay time instead of a 120 second assay was implemented. Walton (2021) found success in identifying trace elements of interest with a 12 mil Al, 1 mil Ti, 6 mil Cu filter and preliminary testing determined that a 12 mil Al, 1 mil Ti, 6 mil Cu filter was successful in yielding clear, defined peaks of lighter elements while still amplifying heavier elements. A 12 mil Al, 1 mil Ti, 6 mil Cu filter was used for this study.

The HHXRF spectrometer was placed in an acrylic stand and positioned upright, allowing for maximum consistency (Figure 3). The device was then connected to a designated PC laptop with the programs S1PXRF and ARTAX, both by Bruker. The S1PXRF program's PC trigger function allows the device to be operated through the computer, as well as displays live spectra as data is collected. The tooth was placed directly on top of the detector beam window, positioned to cover as much area of the window as possible. This ensures the maximum of amount of incident photons come in contact with the tooth (Walton 2021, Bergmann 2018). A protective metal shield was placed over top of the sample while photons were being emitted from the HHXRF device. Two 90 live-second assays were done per surface per tooth to ensure the accuracy of the results and the functionality of the machine. Incisors were assayed on both the palatal surface and labial surface, producing a total of four total spectra per incisor. The occlusal surface and the mesial side of the first molar was assayed, producing a total of



Figure 3: Bruker HHXRF positioned in acrylic stand (Image by Griffon Binkowski)

four total spectra per molar. The second molars were assayed in the same way, yielding a total of four total spectra per molar. The occlusal surface of the third molar was assayed, producing a total of two total spectra per molar. The sides of the third molars were not assayed due to their smaller width and failure to cover the HHXRF device's detection window completely. This was done to prevent the introduction of root cementum into the detection beam when the primary target was crown enamel.

Data Analysis

The collected data was transferred into the ARTAX software for peak visualization and net photon count extraction. ARTAX offers the built in Bayesian Deconvolution process, which assesses the likelihood that a particular element is present within the sample (Bloch 2015). This allows for the results to be given as net intensities or net photons, which are counts of the area under each spectral peak, minus background, minus inter-elemental effects (peak overlapping) (Bloch 2015). All spectra were normalized to the inelastic Compton peak produced by the X-ray tube; these peaks were found at 18.5-19 keV. To assist in visual comparison of peaks, incisor spectra were colored blue, first molar spectra was colored gold, second molar spectra were colored green, and third molar spectra were colored red. Spectra were grouped by individual and overlaid for a visual peak-to-peak comparison.

Net photon counts of Sr, Br, Ca, and P were converted into ratios in order to be compared; this was done because of the absence of a standard. At the group level, an ANOVA test at significance level 0.05 was used to assess variance by tooth type for calculated Ca/P ratios, Sr/Ca ratios, and Br/Ca ratios for all assays. A post-hoc Tukey's test was used to identify specific group differences.

CHAPTER FOUR: RESULTS OF STUDY

Intra-individual Results

Intra-individual Spectral Assays

Spectra for each tooth per individual were compiled, overlaid, and colored for qualitative assessment using the ARTAX software. This allowed for successful direct comparison of tooth spectra per individual. Across all individuals, the Ca $K\alpha$ and associated Ca $K\beta$ peaks were discernable and exhibited peak uniformity in all tooth types, making Ca peaks 100% discernably consistent across all teeth. This is true for the P $K\alpha$ peaks as well, making P peaks 100% discernably consistent across all teeth. Per individual, Sr $K\alpha$ peaks were discernable and stayed relatively consistent in all M3 teeth and all I1 teeth. However, the exception to this consistency is individual AH-E-44/10, who displays discernable differences in I1 between the palatal and labial assays (Fig. 4). This makes Sr peaks 100% discernably consistent in M3 teeth and 93.75% discernably consistent in I1 teeth. Strontium consistencies per individual for M1 stayed relatively consistent, aside from individual AH-K-29/8 who exhibited discernable differences between mesial and crown assays, making Sr peaks 80% discernably consistent in M1 teeth (Fig. 5).

Out of the 10 individuals who possessed an M2 sample, three did not show consistent strontium peaks between the mesial and crown assays. These individuals were AH-C-13/14, AH-C-13/33, and AH-K-35/6 (see Appendix A, Figures 13, 14 and 26 respectively). This makes Sr peaks 81.25% discernably consistent in M2 teeth. In individuals where Sr peaks differed per M1 or M2 tooth, the mesial side produced the higher peaks.

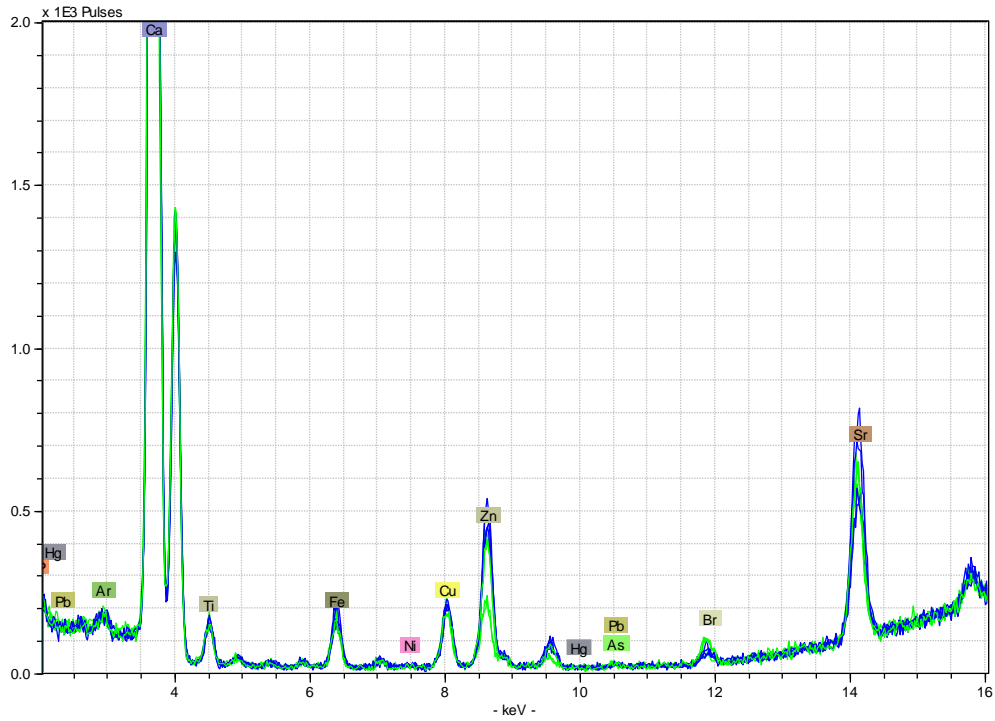


Figure 4: HHXRF spectra of M2 and I1 from individual AH-E-44/10. Br stands for bromine; Sr stands for strontium. Ca stands for calcium. M2 is represented by green, I1 is represented by blue.

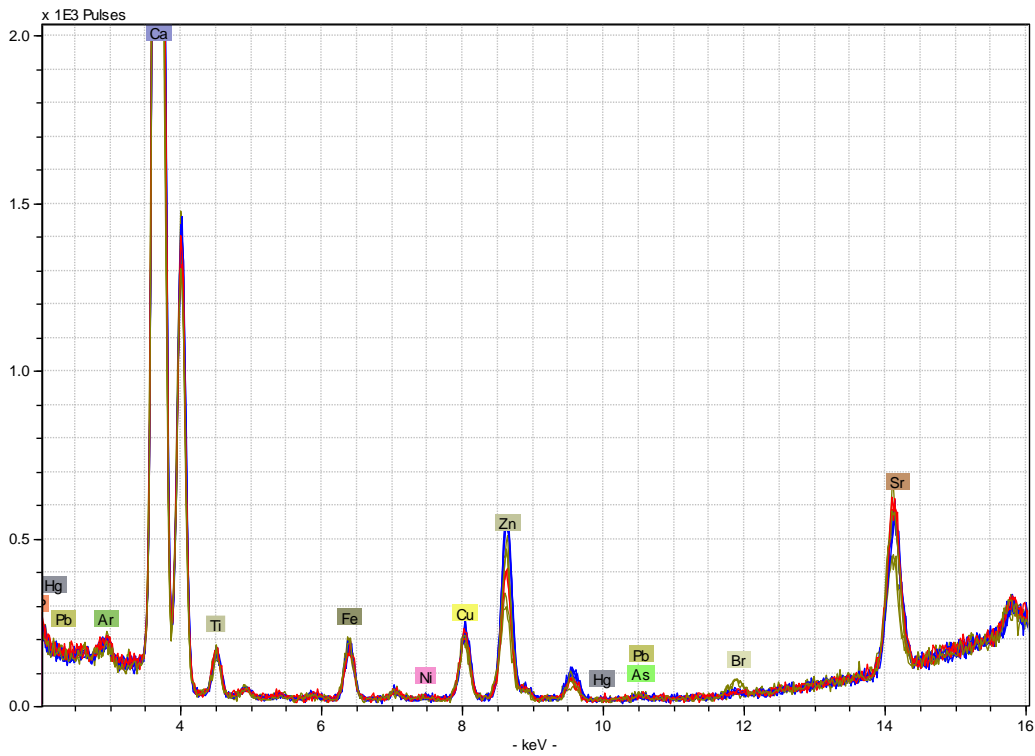


Figure 5: HHXRF spectra of M1, I1, and M3 from individual AH-K-29/8. Br stands for bromine; Sr stands for strontium. Ca stands for calcium. M1 is represented by gold, I1 is represented by blue, and M3 is represented by red.

Per individual, Br $K\alpha$ peaks were discernable, but very small compared to other trace elements of interest. M3 bromine peaks remained relatively consistent throughout all individuals, making Br peaks 100% discernably consistent in M3 teeth. I1 bromine peaks stayed relatively consistent aside from individuals AH E-44/3 and AH-K-35/5, who exhibited discernably different peaks between the mesial and crown assays. This makes Br peaks 87.5% discernably consistent in I1 teeth. Out of the five individuals who possessed an M1 sample, two did not show consistent bromine peaks between the mesial and crown assays. These individuals were AH-K-29/8 and AH-K-29/19 (see Appendix A, Figures 22 and 24 respectively). This makes Br peaks 60% discernably consistent in I1 teeth. The majority of Br peaks in M2 teeth did not show consistent bromine peaks between the mesial and crown assays. Out of the 10 individuals who possessed an M2 sample, only two individuals, AH-E-44/7 and AH-E-44/10, showed consistency, making Br peaks only 20% discernably consistent in M2 teeth (see Appendix A, Figures 18 and 20 respectively). In individuals where Br peaks differed per M1 or M2 tooth, the mesial side produced the higher peaks. However, the peaks of Br are small, so it is difficult to say what constitutes a significant difference between mesial and crown peaks.

Inter-individual Results

Inter-individual results will be presented through qualitative assessments of spectra, boxplots, and strip charts, as well as semi-quantitative statistics.

Inter-individual Qualitative Assessment

The Ca $K\alpha$ and associated Ca $K\beta$ peaks were relatively uniform across all individuals; this is true for the P $K\alpha$ peaks as well. Generally, Sr $K\alpha$ peaks for M3 across individuals were equal to or higher than peaks associated with M1, I1, or M2. There are two exceptions to this trend found

in individuals AH-C-13/14 and AH-C-13/33. Sr peaks for the M1, I1, and M2 teeth vary from individual to individual. Br $K\alpha$ peaks differed per tooth across all individuals, with the only qualitative trend being little to no discernable peaks for M3 samples.

Extracted net photons for each assay per tooth per individual were converted into a ratio. However, assays that exhibited photon counts ≤ 5 were excluded from analysis as these would produce extreme outliers. Out of 146 assays, eight assays meeting these criteria were removed from analysis (see appendix B). Calculated ratios were then expressed as sets of boxplots; one boxplot was created per tooth. The Ca/P boxplots show relatively little fluctuation between teeth with a relatively stable minimum and maximum values per tooth (Figure 6).

The Sr/Ca boxplots show a clear upwards trend between teeth. Two tooth samples appear to be outliers in the M2 column, while one outlier appears to be present in the M3 column. Two overlapping circles represents the first and second assay per side per tooth (Figure 7).

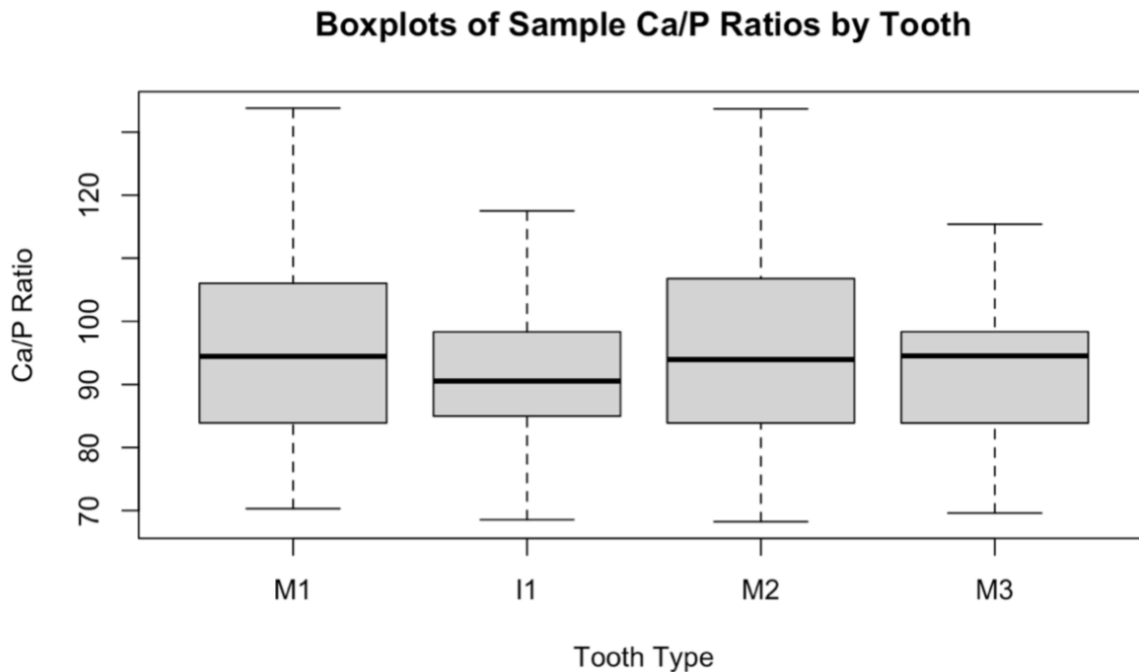


Figure 6: Boxplots of sample Ca/P ratios organized by chronological formation of each tooth.

The Br/Ca boxplots show different ratios across all teeth. M2 has a high maximum compared to the other teeth, and its median falls closer to the low side of the inter quartile range. I1 exhibits three outlier values, with two in the middle overlapping to represent a single side of the I1 tooth. M3 also exhibits an outlier, though it is closer to the maximum value than outliers from I1 (Fig. 8).

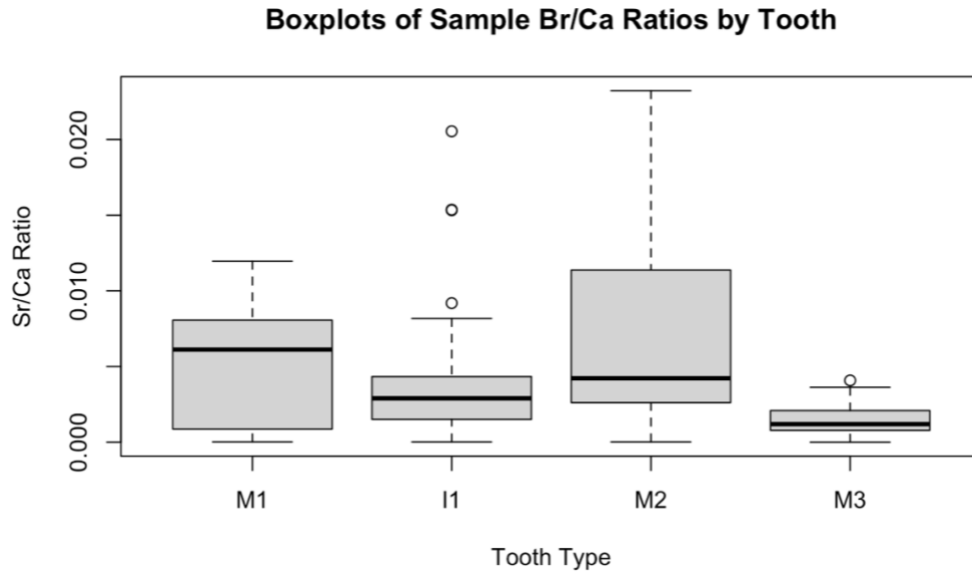


Figure 7: Boxplots of sample Sr/Ca organized by chronological formation of each tooth.

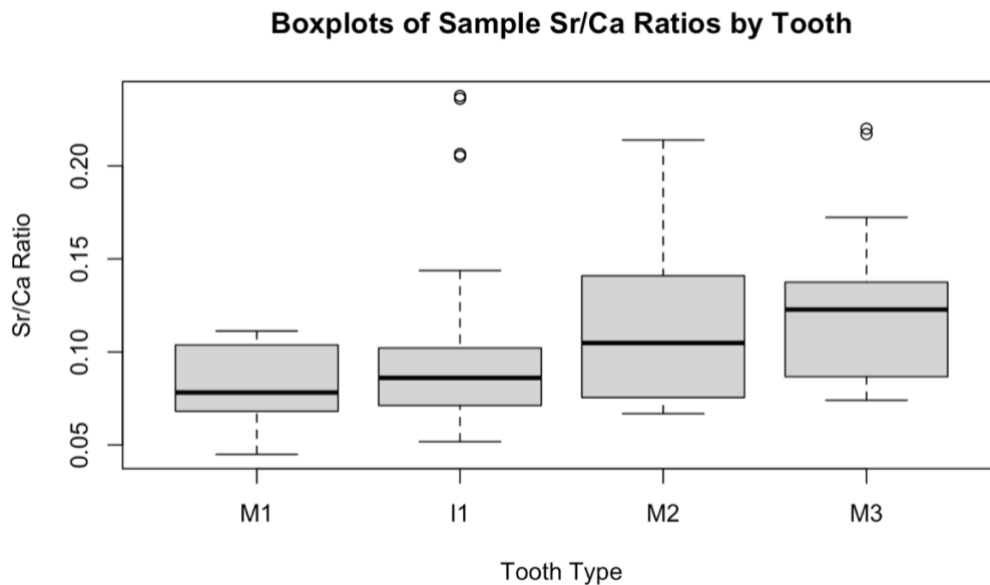


Figure 8: Boxplots of sample Br/Ca ratios organized by chronological formation of each tooth.

Trace element ratios considered diet and mobility indicators were averaged per tooth for each individual and fitted to strip charts. One strip chart was created per trace element ratio. The Sr/Ca strip chart displayed a general upward trend in ratio values across tooth development periods. However, some individuals do not fit this pattern, such as individual AH-C-13-33, who exhibits a discernably smaller Sr/Ca ratio from the M2 tooth to the M3 tooth (Figure 9). The Br/Ca shows a pattern of rising and falling values from tooth to tooth. Most individuals adhere to this pattern, with AH-K-35/5 being and AH-E-44/7 being the exceptions. In individual AH-K35/5, instead of the Br/Ca ratio decreasing from M1 to I1, it instead increases. In individual AH-E-44/7, there is a slight increase in the Br/Ca ratio from M2 to M3 (Figure 10).

Inter-individual Semi-Quantitative Statistics

An ANOVA test was used to assess if any differences in ratio means existed between tooth groups per trace element ratio of interest. In these tests, individuals were pooled so that only the tooth group was the primary factor in determining possible variance. The alpha level was set at 0.05 and a post hoc Tukey's test was used to specify which tooth groups showed variability (see Table 3 for ANOVA and Tukey's p-values). The ANOVA test performed on the Ca/P ratios yielded a p-value = 0.335 for all teeth, showing that tooth type did not significantly impact Ca/P ratios per tooth group. The ANOVA test performed on the Sr/Ca ratios yielded a p-value = 0.000788 for all teeth, showing that tooth type did significantly impact Sr/Ca ratios per tooth group. The Tukey's test revealed differences between M1-M2, I1-M3, and M1-M3 groups. The ANOVA test performed on the Br/Ca ratios yielded a p-value = 4.15e-05 for all teeth, showing that tooth type did significantly impact Br/Ca ratios per tooth group. The Tukey's test revealed differences between I1-M2, M2-M3, and M1 -M3 groups.

Sr/Ca Ratio Means of Individuals from Altun Ha, Belize

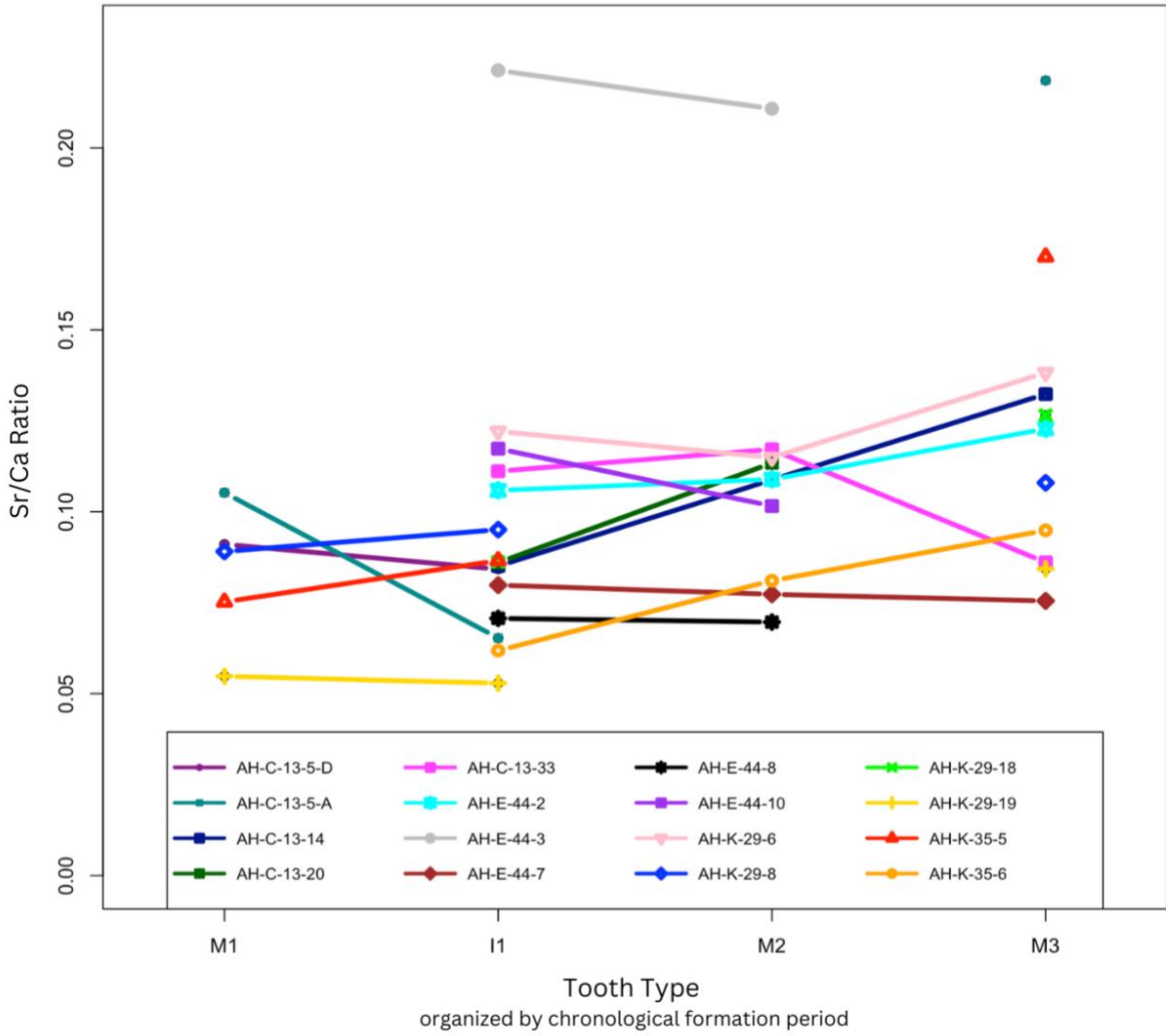


Figure 9: Strip chart of Sr/Ca ratio means of all individuals from the sample.

Br/Ca Ratio Means of Individuals from Altun Ha, Belize

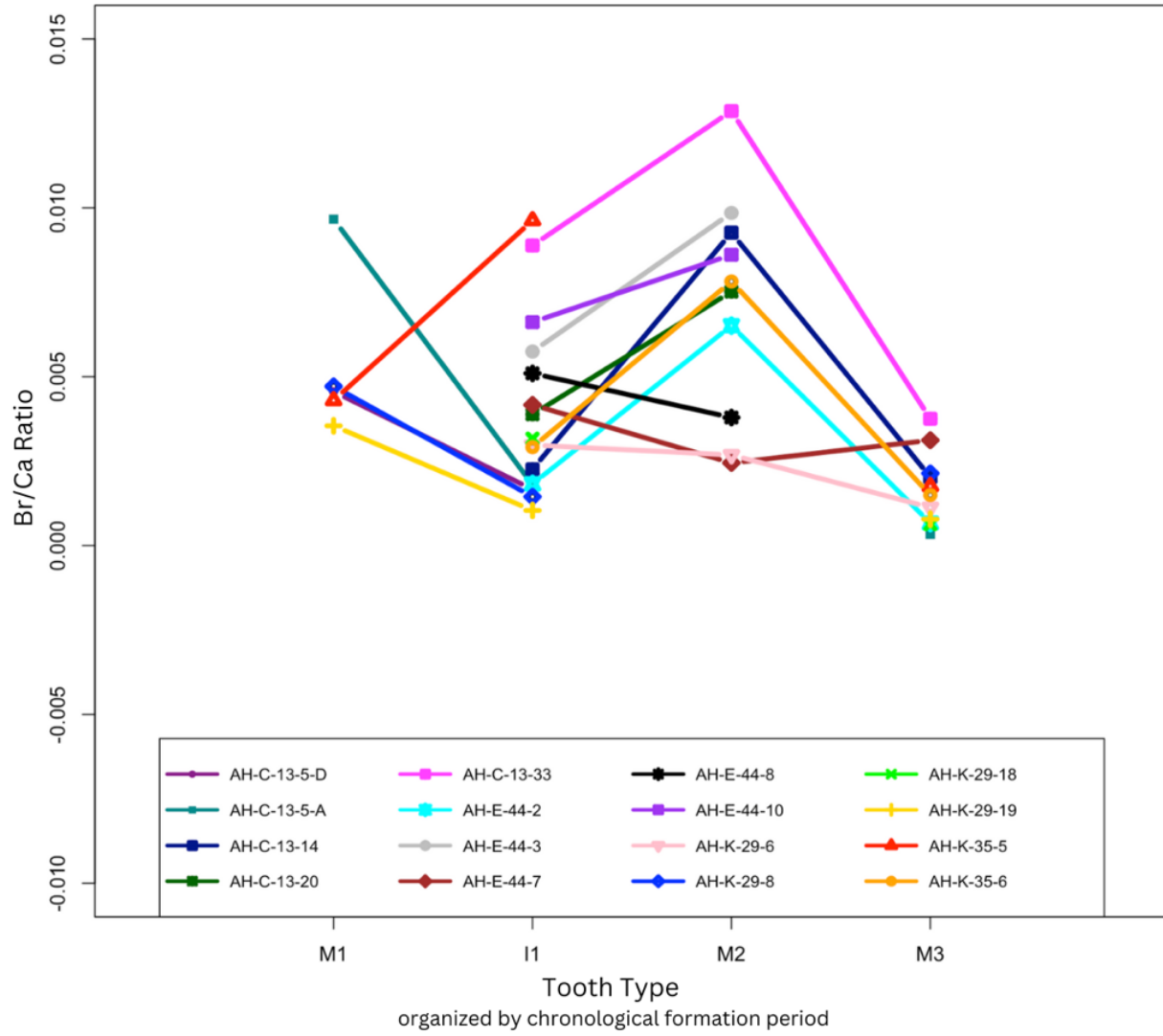


Figure 10: Strip chart of Br/Ca ratio means of all individuals from the sample.

Table 3:ANOVA and Tukey's test results for trace element ratios of interest. Significant p-values are bolded.

	CA/P RATIOS	SR/CA RATIOS	BR/CA RATIOS
ALL TEETH	0.335	0.000788	4.15E-05
M1-I1	0.415889	0.5173962	0.3302843
I1-M2	0.5991572	0.1161918	0.0021035
M2-M3	0.7721964	0.7860551	0.000068
M1-M2	0.9757596	0.0151924	0.5641537
I1-M3	1	0.0212384	0.2161344
M1-M3	0.5954313	0.0027825	0.0173282

CHAPTER FIVE: DISCUSSION OF RESULTS

Implying Diet and Mobility

Insights Gained from Strontium

Diets at Altun Ha consisted of the staple carbohydrate maize, as well as a large marine component due to its proximity to the ocean (White et al. 2001). Ca/P ratios did not exhibit any significant difference between tooth groups ($p = 0.335$), which was expected as calcium phosphorous ratios in hydroxyapatite remain relatively stable. In a sample-wide comparison of Sr/Ca ratios, there is a notable steady increase in Sr/Ca ratios over tooth developmental periods. This is shown through boxplots, strip charts, and a Tukey's test which identified significant differences in the M1-M2 tooth groups ($p < 0.05$), I1-M3 tooth groups ($p < 0.05$), and the M1-M3 tooth groups ($p < 0.005$). Marine substance sources have been shown to have more trace element strontium than terrestrial subsistence sources, with the exception of nuts. (Pate 1994). Additionally, breast milk consumption produces a trophic-level effect, placing breast feeding children at a higher trophic level and results in low strontium readings in dietary studies (White et al. 2001). Thus, a gradual chronological increase in Sr/Ca ratios was expected as childhood weaning periods conclude, and children begin to consume local marine subsistence sources.

Sr spectra consistency remained relatively stable for all measurements of the teeth, making false elevated Sr peaks unlikely. Although Ramon nuts were identified as a part of the diet at nearby Maya site Lamanai, there is little evidence to suggest Ramon nuts made up most of the diet (White et al. 1988). This can be applied to Altun Ha where there is more evidence for a large marine component to the diet, making elevated Sr/Ca ratios attribution to intense Ramon nut consumption unlikely. Although a high consumption of plant life is associated with high

trace element strontium in tooth and bone, the major staple crop of maize is known to exhibit comparatively lower strontium levels (Simpson et al. 2021). This makes the possibility of maize being responsible for high Sr/Ca ratios unlikely. Thus, a gradual chronological increase in Sr/Ca ratios can most likely be attributed to increased intake of marine sources post-weaning. This aligns with previous isotopic results for the individuals of Altun Ha, where evidence implies a heavy intake of marine resources (White et al. 2001).

An inter-individual approach reveals a notable outlier in the sample. Individual AH-E-44/3 exhibits Sr/Ca ratios far more elevated than the rest of the individuals in the I1 and M2 tooth groups. This could imply that this individual is not from Altun Ha or consumed different subsistence sources than the other individuals in the sample. Additionally, individual AH-C-13/5 also exhibits an elevated M3 Sr/Ca ratio, as does individual AH-K-35/5. However, a more nuanced investigation is needed to fully explain these differences and is beyond the scope of this study.

Insights Gained from Bromine

As previously mentioned, bromine remains a highly debated trace element for use in implying diets of past people (Kozachuk et al. 2020, Dolphin et al. 2013). The presence of bromine peaks was expected in this sample because of the large marine component in the diet of individuals at Altun Ha (White et al. 2001). Across all teeth in all individuals, bromine peaks and Br/Ca ratios were discernable, but very small. The range for Br/Ca ratios ranged from 0 to 0.025. However, values did differ from tooth to tooth as the Tukey's test p-values indicate. On a whole sample level, the data displays about even ratios of Br/Ca in M1 and I1, with an increase in M2, and then a final decrease in M3. This could be due to two factors: diet change and/or mobility, or introduction of cementum into the HHXRF beam.

Some dietary components contain higher amounts of bromine than others. One dietary component that contains high bromine levels are marine organisms, such as seaweed, mollusks, and some fish (Dolphin et al. 2013). Bromine can also contaminate foods by the sea spray effect, whereby seawater molecules combine with nearby terrestrial food sources (Wytttenbach et al. 1997). Animals that consume high amounts of brominated organisms can also produce high bromine levels. Bromine is also found in relatively high amounts in human breast milk, with an increase in bromine occurring around 2 months post-partum (Mohd-Taufek et al. 2016). Notably, a post hoc test identified discernable differences between the I1-M2 tooth groups ($p < 0.005$) and M2-M3 tooth groups ($p < 0.001$). Fluctuations in Br/Ca ratios per tooth group may reflect bioaccumulation of bromine due to dietary shifts, such as a post-weaning transition from high Br breast milk to higher Br marine resources. This is possible for the I1-M2 tooth group, where the final enamel formation period of I1 aligns with the end of weaning age in Altun Ha (White et al. 2001). A significant difference may also be explained by dietary change whereby the availability of brominated foods was either more or less accessible.

However, the second possible explanation of differing Br/Ca values may attribute these shifts to methodological issues. As reported in the results of this study, Br had low assay continuity between the mesial and crown surfaces of selected molar samples (M1 = 60%, M2 = 20%). The mesial side of molars consistently produced higher bromine peaks and net photon counts. This is possibly due to the distribution of Br within the tooth, or the intrusion of cementum into the incident photon beam. Previous studies mapping the concentration of bromine in teeth found most of the present Br is stored within the cementum due to the element's affinity for the organic parts of skeletal tissue, though a small portion (.01%) is found in the inner crown enamel (Dolphin et al. 2013, Mariel et al. 2014). This makes a high bromine concentration in the

sides of the tooth enamel an unlikely explanation. A Tukey's test also revealed that there was no significant difference in M1 and M2 tooth groups ($p=0.564$). These tooth groups were the only groups to be assayed on the crown and mesial side of the tooth; M3 was only assayed on the crown due to lack of side width. It is possible that parts of the cementum entered the incident photon beam during scanning, creating a higher peak and net photon count for bromine on the mesial side of the molars.

An inter-individual approach also corroborates this possibility. All individuals noted to have displayed inconsistent peaks per mesial and crown set of scans for M2 exhibit a high Br ratio mean displayed in the constructed strip chart (see Figure 10). As Sr/Ca ratios were averaged per tooth, these ratio means may have been artificially higher instead of representing the true average ratio mean of the enamel. However, an intra-individual approach also displays variation in Br levels per tooth groups and between tooth groups. For example, the Br/Ca ratio mean of individual AH-K-35/5 increases from M1 to I1, while all other individuals in that group exhibit a decline in Br/Ca ratios. This may indicate that there are other factors that may influence the difference in Br/Ca ratios.

With both explanations presented, results are too inconclusive to attribute shifts in Br/Ca ratios to any one factor. However, the cause of these shifts warrants further investigation, which is beyond the scope of this study.

Social Complexity in Altun Ha

Though notable trends have been identified for trace element ratios of interest, an intra-individual model has aided in revealing the complexities of these trends. A sample-wide assessment of trends may occlude the variability within an individual's life, and by extension, the community of Altun Ha. A gradual increase in Sr/Ca ratios over developmental time was

discerned, but several individuals do not adhere to this model. Specifically, individuals AH-E-44/7, AH-C-13/13, C-13/5A and AH-E-44-10 all exhibit discernable decreases in Sr/Ca as their dental developmental periods progress (see Figure 9). Altun Ha is known to have been a highly complex and active social center. Trade existed with other Maya polities, high elites and lower status elites are known to have occupied Altun Ha, and noted dietary and cultural differences are associated with gender and status (White et al. 2001). It is also notable that White et al. (2001) wrote that individuals from the C zone are believed to not be from Altun Ha. Though it is beyond the scope of this study, unraveling complexities such as this will continue to be investigated by using this intra-individual model, which shows to be promising when researching complex lifeways at Altun Ha.

Applications of HHXRF in Bioarcheology

Diet, mobility, toxicity exposure, and general health are subjects integral to the field of bioarcheology. Studying these aspects of a past individual or group helps researchers better understand past societies and our transition to today. However, many methods of analysis require destructive preparation or assay tactics. Inductively Coupled Plasma Mass Spectrometry (ICP-MS) often requires homogenization of a sample. This results in skeletal tissue being cut, demineralized, and ground into a powder fit for analysis. Laser Ablation Inductively Coupled Plasma Mass Spectrometry (LA-ICP-MS) utilizes a plasma laser to create an aerosol of molecules from a small part of the sample for analysis. Though sample alteration is less than ICP-MS, it still removes a portion of the sample, and is thus still destructive (Simpson et al. 2021). This destruction can not only be detrimental to a collection but can be perceived as disrespectful and intrusive by descendant communities.

Today, anthropologists must be cognizant that skeletal remains were once people, and to some, still are. Remains are intrinsically tied to a once living person and great care must be taken to respect this while continuing scientific inquiry. An ideal way to respect the humanity of skeletal remains and further scientific knowledge is the implementation of non-destructive methods of analysis, such as HHXRF. There is opportunity for HHXRF to be utilized more in bioarcheology. Future studies would benefit from its non-destructive nature, as well as its relatively low sample preparation and cost. Application of HHXRF in the field would also be beneficial, allowing for improved prioritization of samples of interest and preliminary sorting of samples. Investigations into the logistics of these potential practices is beyond the scope of this study but warrants further attention in future research.

To summarize, HHXRF has the potential to be used more frequently as an analysis technique to mitigate destruction of bioarcheological samples, preserving collection integrity and descendant community relations while still furthering scientific inquiry.

CHAPTER SIX: CONCLUSIONS AND FUTURE RESEARCH

This study was able to utilize Sr/Ca ratios to imply a diet high in marine subsistence sources from sampled individuals of Altun Ha, Belize using Hand Held X-ray Fluorescence spectrometry. Additionally, this study adds to the growing literature around HHXRF's use in bioarchaeology as a tool to discern trace element signatures related to lifeway activities. Due its recent affirmation as a viable method of analysis for use on bone and teeth, there is little standardization of tube setting, assay times, and appropriate filter use (Bergmann 2018). This study adds to the growing literature outlining methodology used in this regard.

This study also applied an intra-individual and inter-individual method of analysis by employing teeth with different enamel formation periods, allowing for a more nuanced look at individual's early life histories at Altun Ha. Discernable trends per individual were able to be identified. An intra-individual method has been traditionally used in stable isotope studies, but no known HHXRF studies employing this method are known to date (Simpson et al. 2021). Subsequently, this study adds to the literature as being one of the first HHXRF studies to employ an intra-individual model utilizing qualitative and semi-quantitative analyses of archeological tooth enamel.

This study also employed Br/Ca ratios as possible indicators of marine diet. Although there was not enough evidence to definitively imply diet from Br/Ca ratios, fluctuations at the intra-individual and inter-individual warrant further investigation, which is beyond the scope of this study.

The results of this study have contributed to the field of biological anthropology by further establishing HHXRF as an appropriate method of analysis for use on archaeological bone and teeth, as well as outlines methodological methods of collecting data. This continues growing

efforts in biological anthropology to use non-destructive methods of analysis, which works to maintain skeletal collections and encourage positive connections between anthropologists and descendant communities. Additionally, the use of the trace element bromine turned attention to its status as a highly debated trace element dietary indicator. Results of variable values in this study continue to encourage discussion and further investigation into bromine as a dietary indicator, as well as other alternative trace elements. Furthermore, an intra-individual model utilizing qualitative and semi-quantitative analyses of archeological tooth enamel was employed in this study. An introduction of this method of analysis could provide more nuance to future bioarcheological HHXRF studies by highlighting trends within individuals that may be occluded by an entire-sample approach alone.

Study Limitations

One of the main limitations of this study was the number of selected samples. Due to time limitations, sample availability, and sample preservation, individuals were only represented by two or three teeth each. Ideally, all selected individuals would have their M1, I1, M2, and M3 teeth included in this study to assess intra-individual and inter-individual trace element trends more thoroughly. Considering this, a possible error arises. Because M1 values only come from 37.5% of the sample, it may be that only a partial picture of M1 trace element presence was constructed. A possible remedy to this would be to include more M1 teeth in future studies. Additionally, this sample was comprised of 16 individuals total, with 12 individuals classified as adult biological females and possible females, three individuals classified as adult biological males, one individual classified as being of indeterminate sex. White et al. (2001) reported that there are noted differences in diet between biological males and biological females. With female and possible female individuals occupying 75% of the total sample, this data is heavily skewed

towards representing female diet and mobility at Altun Ha. Known diet variation between sexes and a biologically female-heavy sample may not accurately represent diet and mobility of all sexes at Altun Ha. A remedy to this would be to include more samples of biologically determined males to better all individuals at Altun Ha.

Future Directions

A possible future direction includes repeating the procedures of the present study on an increased sample size of individuals from Altun Ha, Belize. Expanding the size of both the number of teeth samples and number of individuals included would produce a wider range of trace element values. Future analyses using this expanding sample size could potentially be more representative of trends observed at the intra-individual and inter-individual level. Additionally, possible future research could explore bromine as a dietary indicator more thoroughly.

Alterations to the methodology utilized in the present study could be done to investigate this trace element in more detail. This could include adjusting voltage and current settings of the HHXRF device, introduction of different HHXRF colored filters, or assay length. Furthermore, only crown enamel could be assayed to mitigate any possible intrusion of cementum into the HHXRF incident photon beam.

Another possible future direction would be to introduce an additional sample group from an inland region. This introduction would allow for a relative comparison of results from non-coastal and coastal populations, further establishing trace element signatures for populations of known dietary intake. The creation of a standard for tooth enamel of a sample group would allow for more precise calibration of the HHXRF device. Empirical calibration curves for each trace element of interest could be created by statically comparing known standards of bone.

APPENDIX A: HHXRF SPECTRA

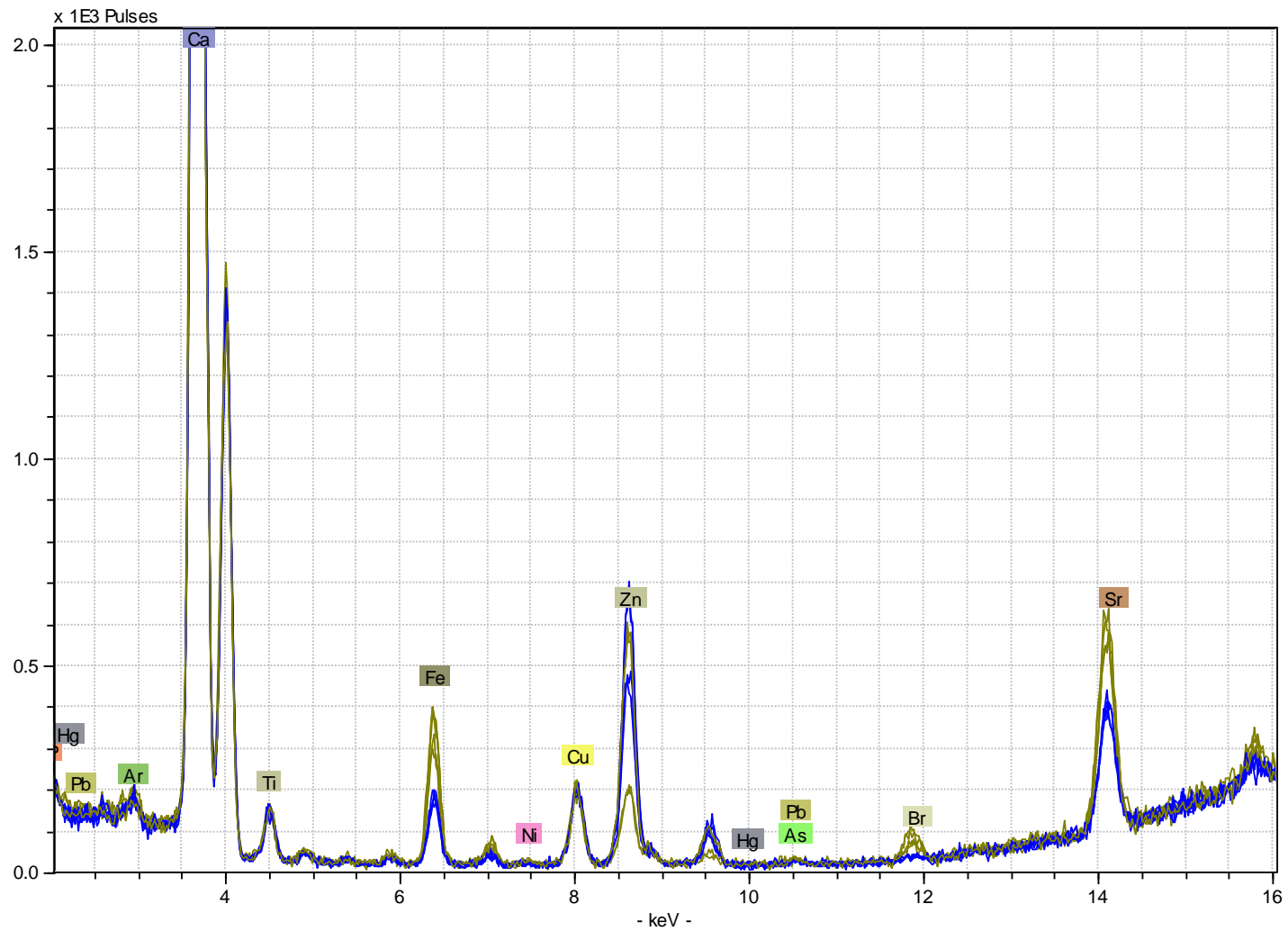


Figure 11: HHXRF spectra of I1 and M1 from individual AH-C-13/5 A. Br stands for bromine; Sr stands for strontium. Ca stands for calcium. M1 is represented by gold, I1 is represented by blue.

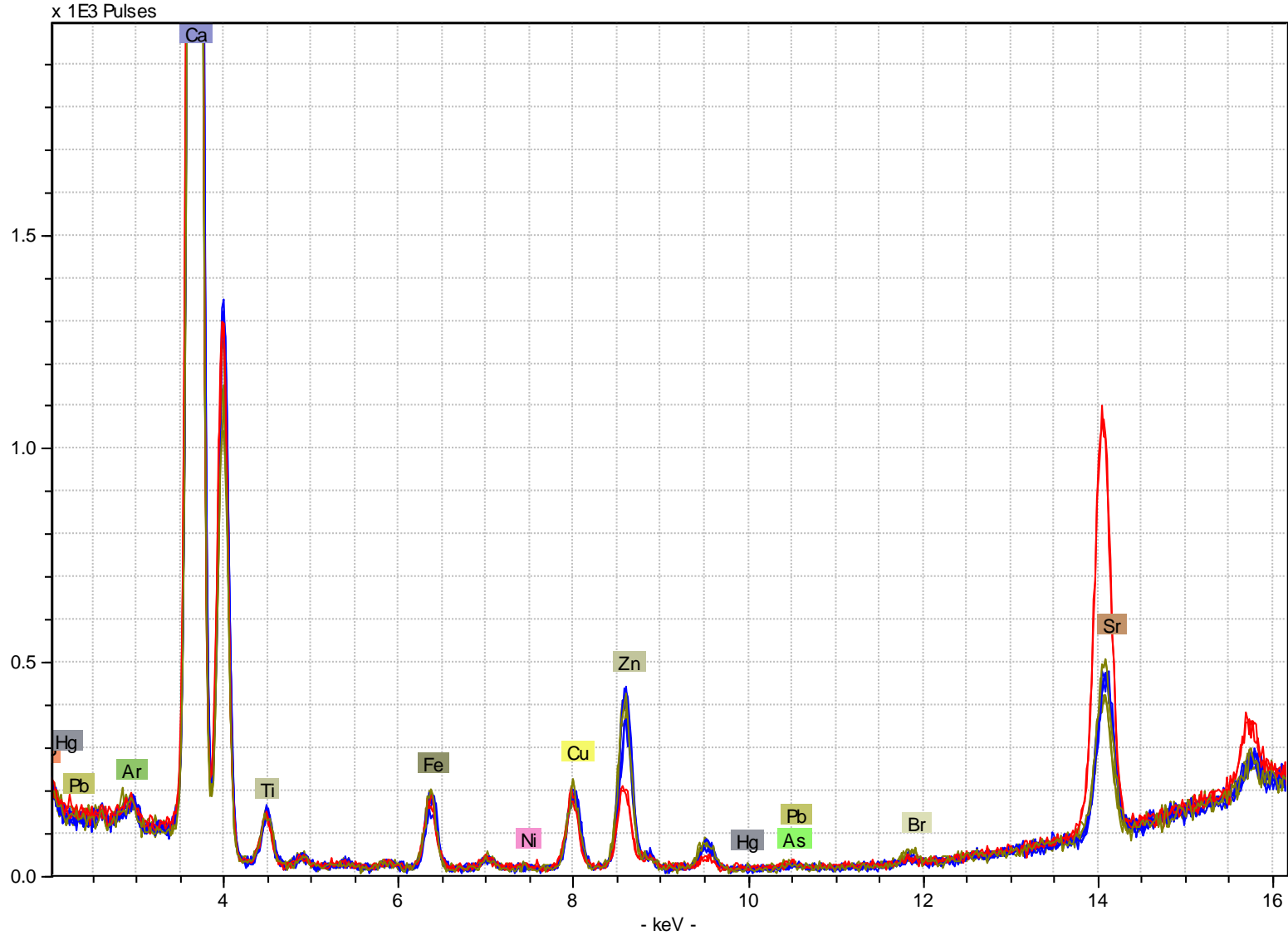


Figure 12: HHXRF spectra of I1 and M1 from individual AH-C-13/5 D. Br stands for bromine; Sr stands for strontium. Ca stands for calcium. M1 is represented by gold, I1 is represented by blue, and M3 is represented by red.

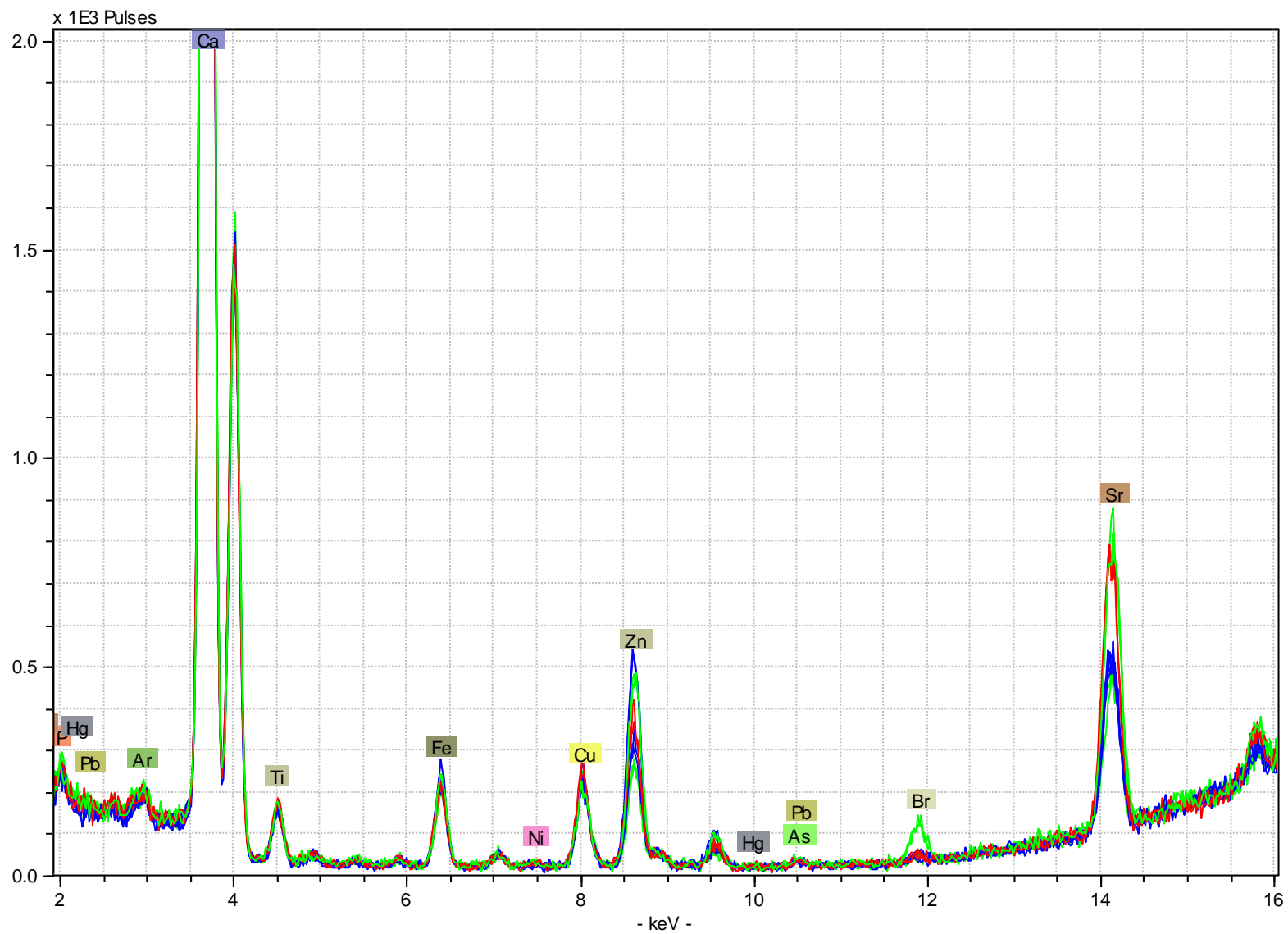


Figure 13: HHXRF spectra of M2, I1, and M3 from individual AH-C-13/14. Br stands for bromine; Sr stands for strontium. Ca stands for calcium. M2 is represented by green, I1 is represented by blue, and M3 is represented by red.

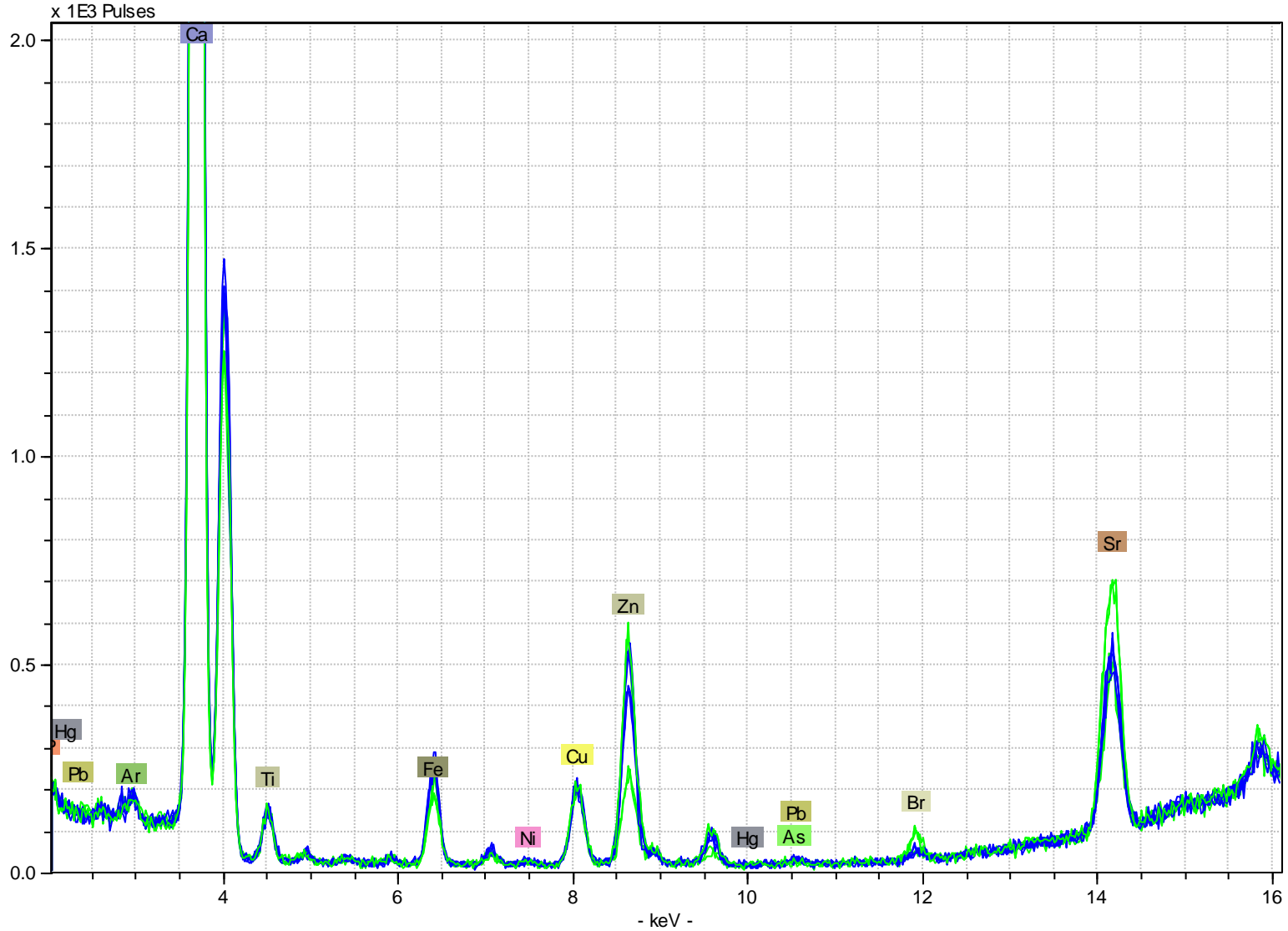


Figure 14: HHXRF spectra of M2 and I1 from individual AH- C-13/20. Br stands for bromine; Sr stands for strontium. Ca stands for calcium. M2 is represented by green, I1 is represented by blue, and M3 is represented by red.

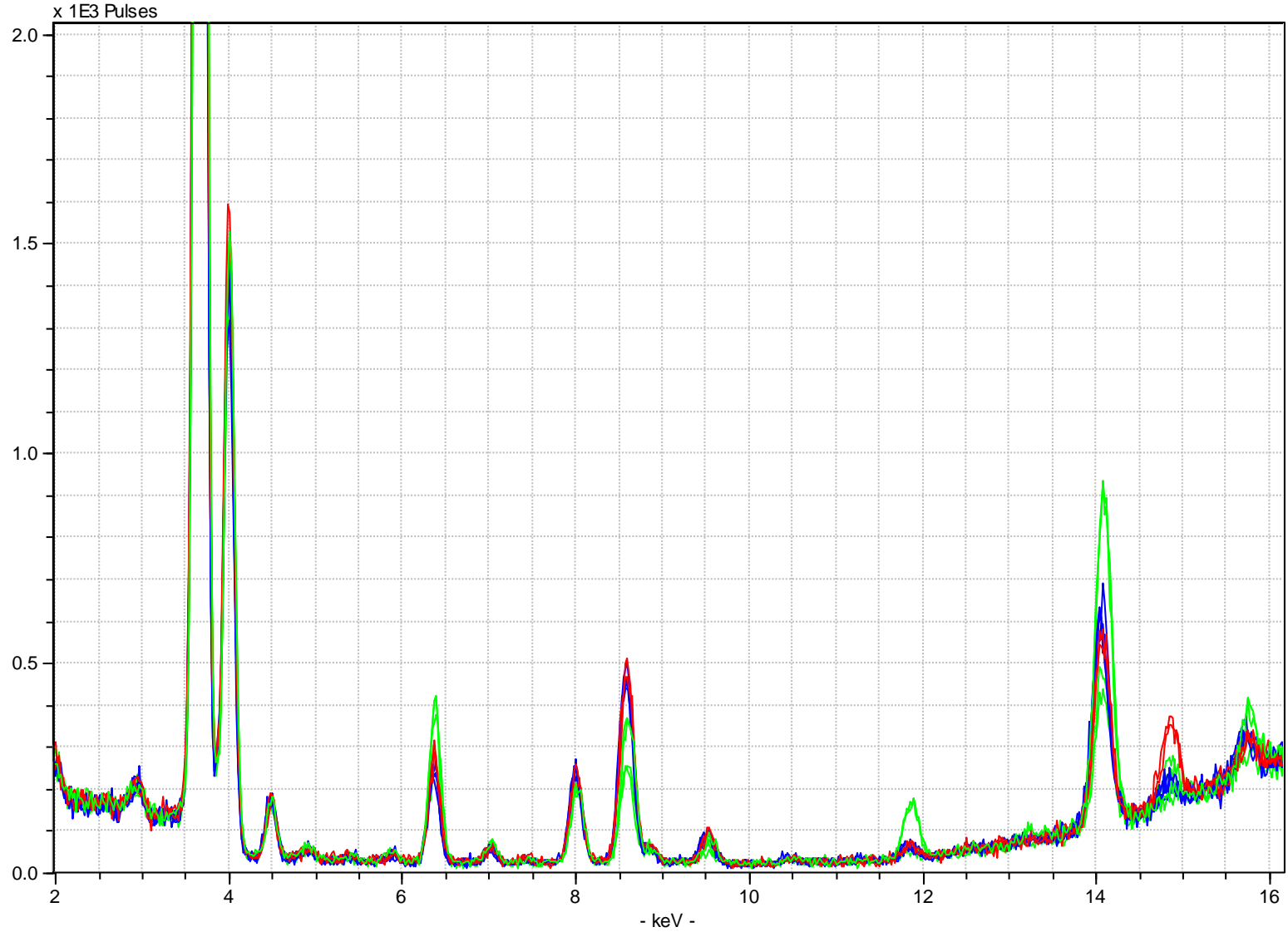


Figure 15: HHXRF spectra of M2, I1, and M3 from individual AH-C-13/33. Br stands for bromine; Sr stands for strontium. Ca stands for calcium. M2 is represented by green, I1 is represented by blue, and M3 is represented by red.

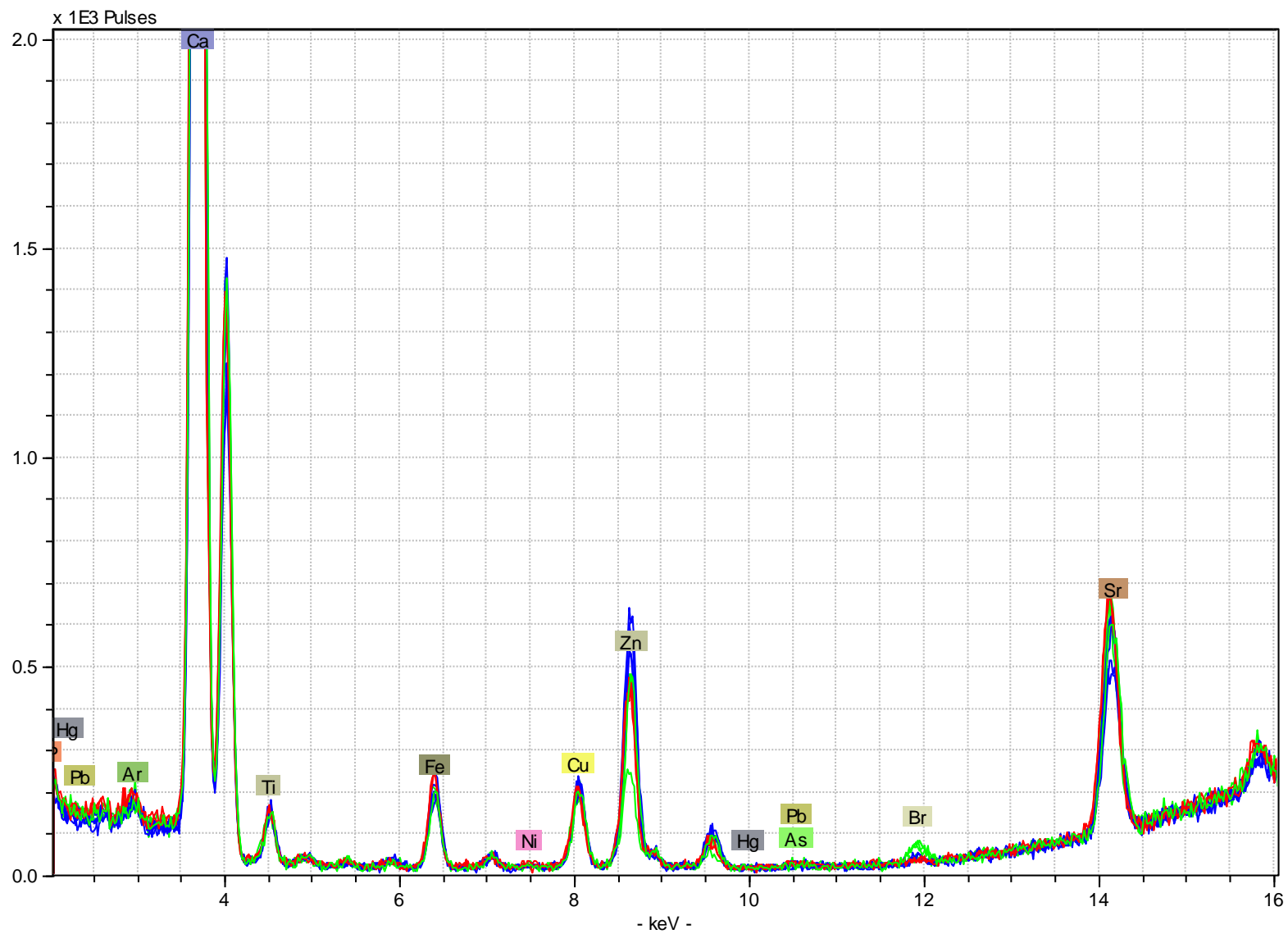


Figure 16: HHXRF spectra of M2, I1, and M3 from individual AH-E-44/2. Br stands for bromine; Sr stands for strontium. Ca stands for calcium. M2 is represented by green, I1 is represented by blue, and M3 is represented by red.

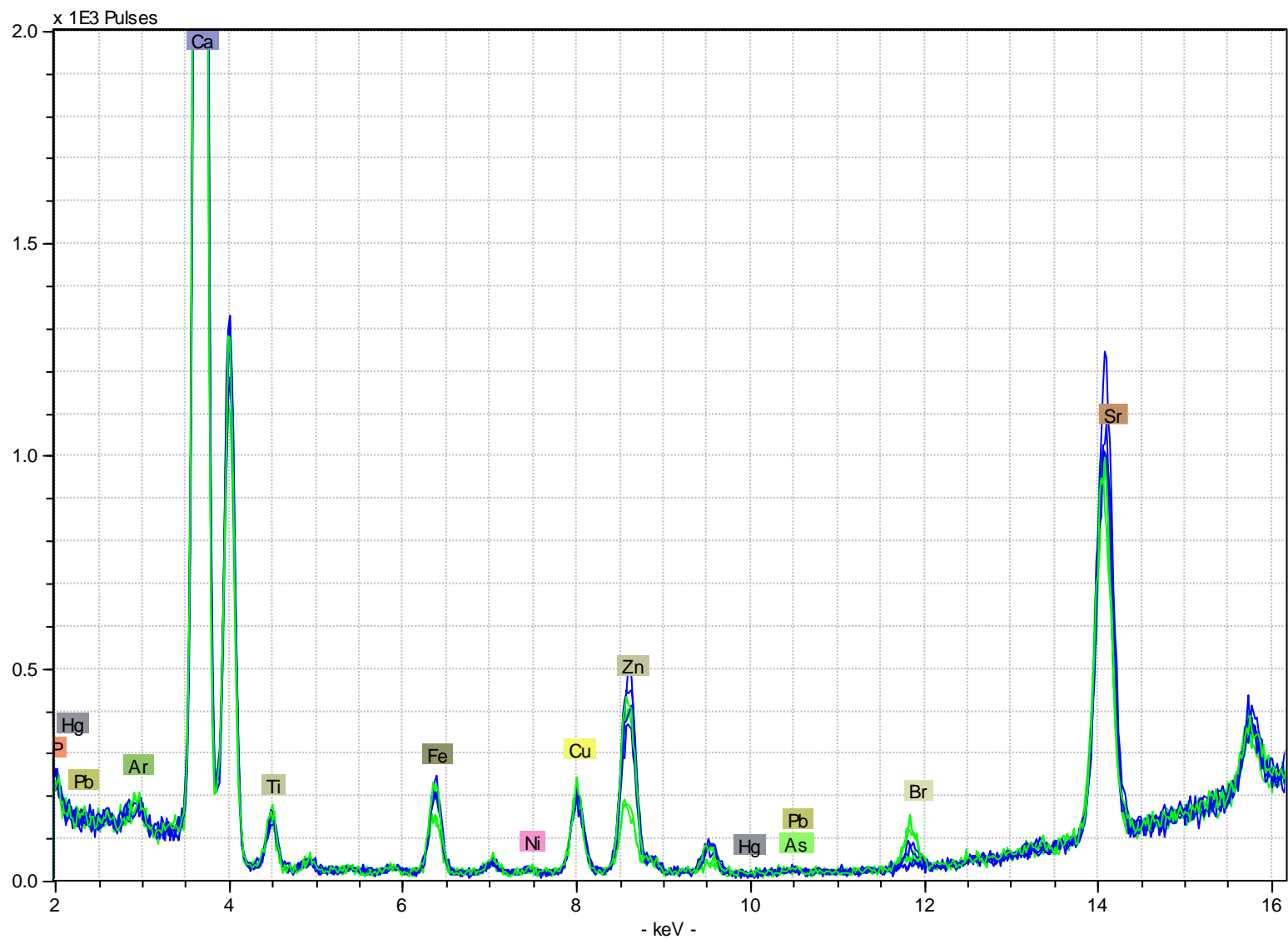


Figure 17: HHXRF spectra of M2 and I1 from individual AH-E-44/3. Br stands for bromine; Sr stands for strontium. Ca stands for calcium. M2 is represented by green, I1 is represented by blue.

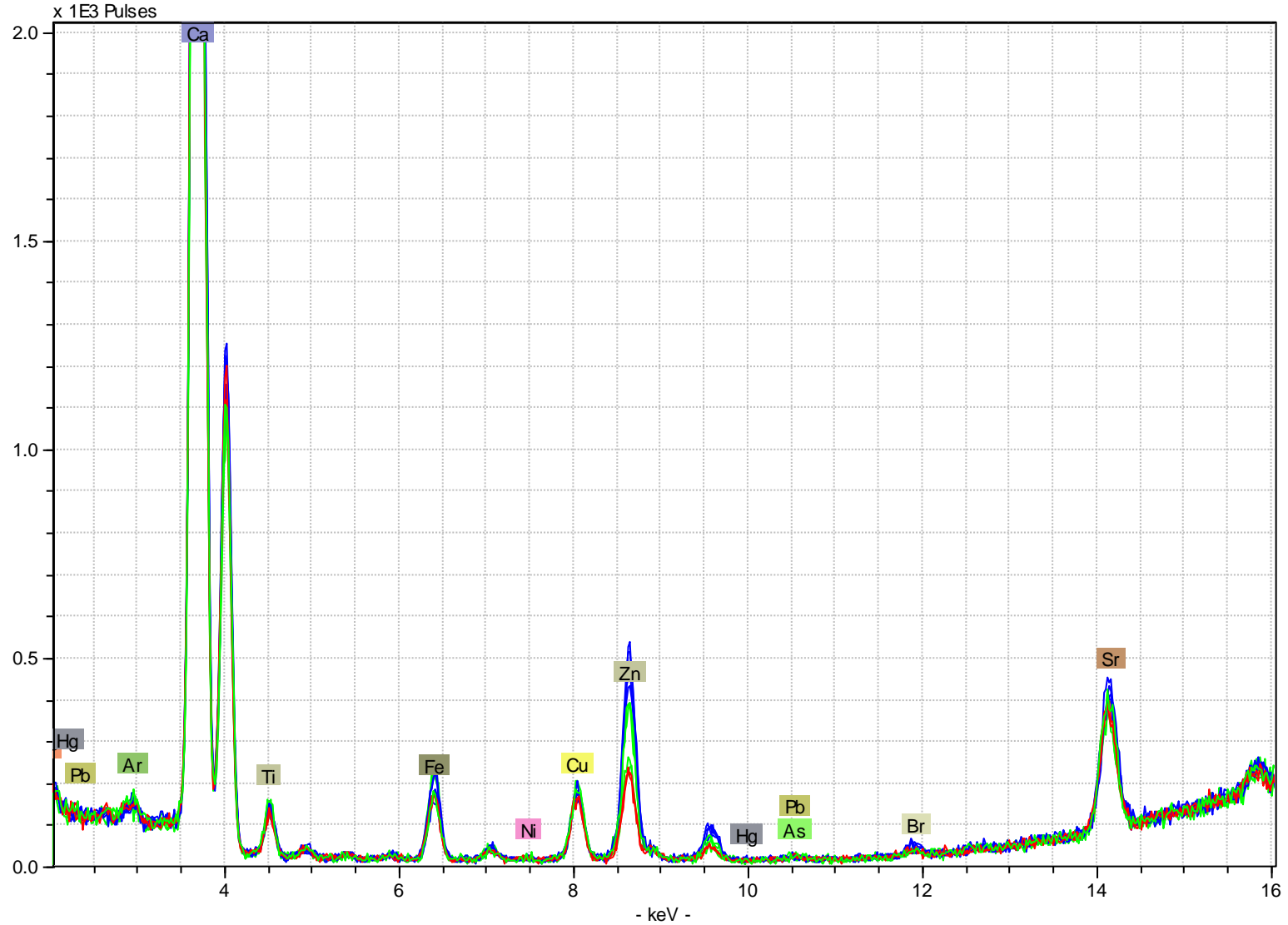


Figure 18: HHXRF spectra of M2, I1, and M3 from individual AH-E-44/7. Br stands for bromine; Sr stands for strontium. Ca stands for calcium. M2 is represented by green, I1 is represented by blue, and M3 is represented by red.

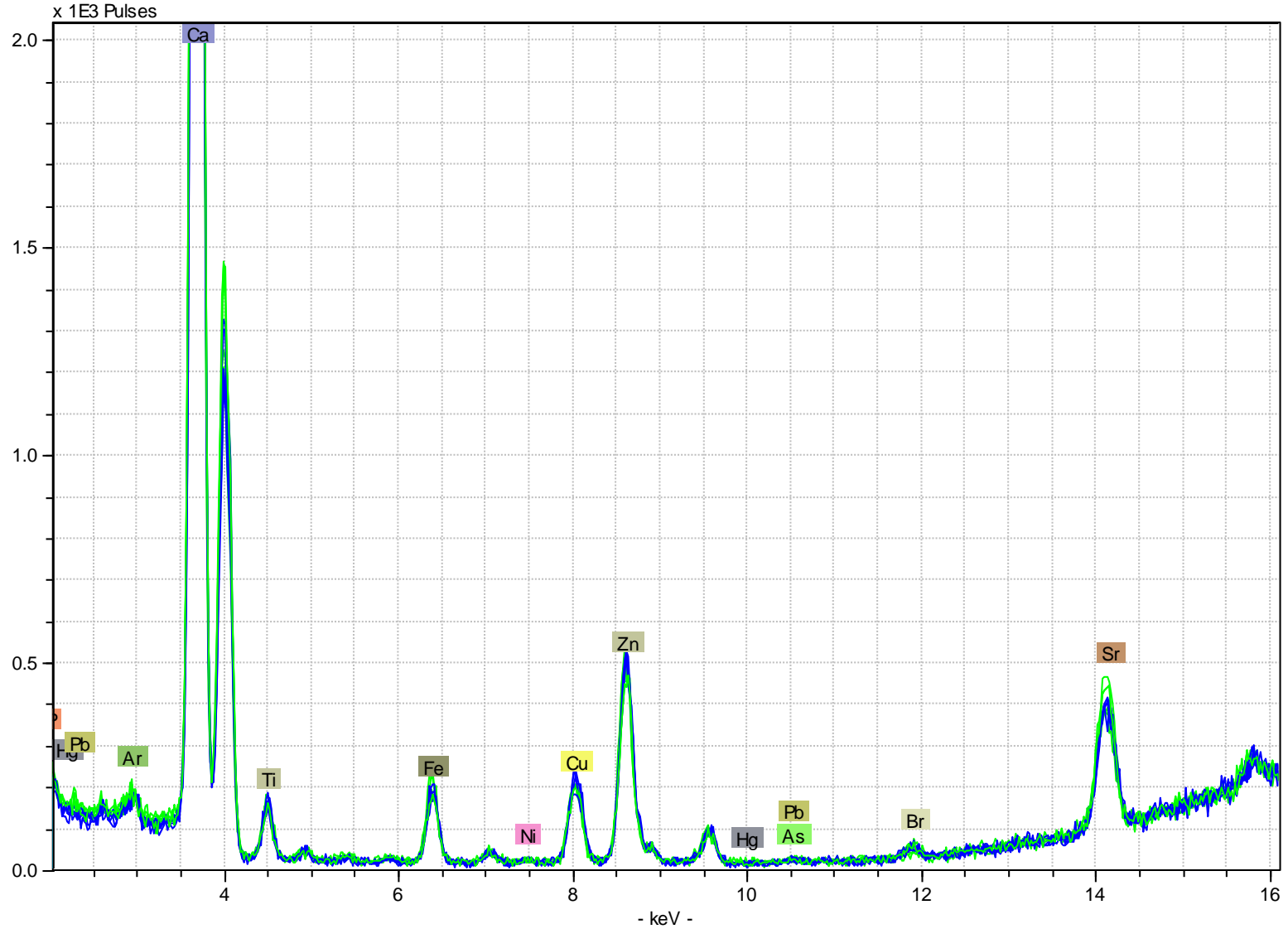


Figure 19: HHXRF spectra of M2 and I1 from individual AH-E-44/8. Br stands for bromine; Sr stands for strontium. Ca stands for calcium. M2 is represented by green, I1 is represented by blue.

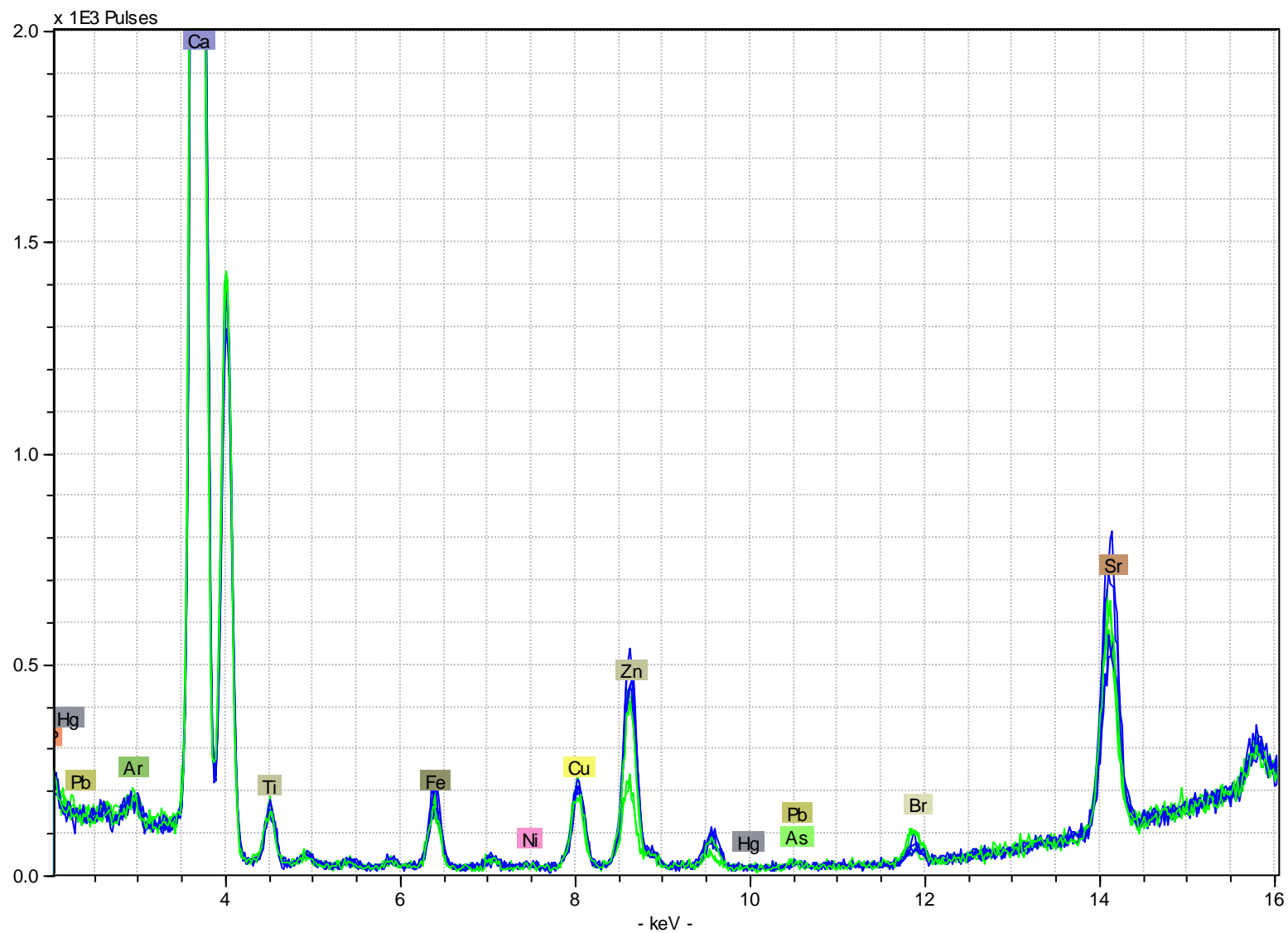


Figure 20: HHXRF spectra of M2 and I1 from individual AH-E-44/10. Br stands for bromine; Sr stands for strontium. Ca stands for calcium. M2 is represented by green, I1 is represented by blue.

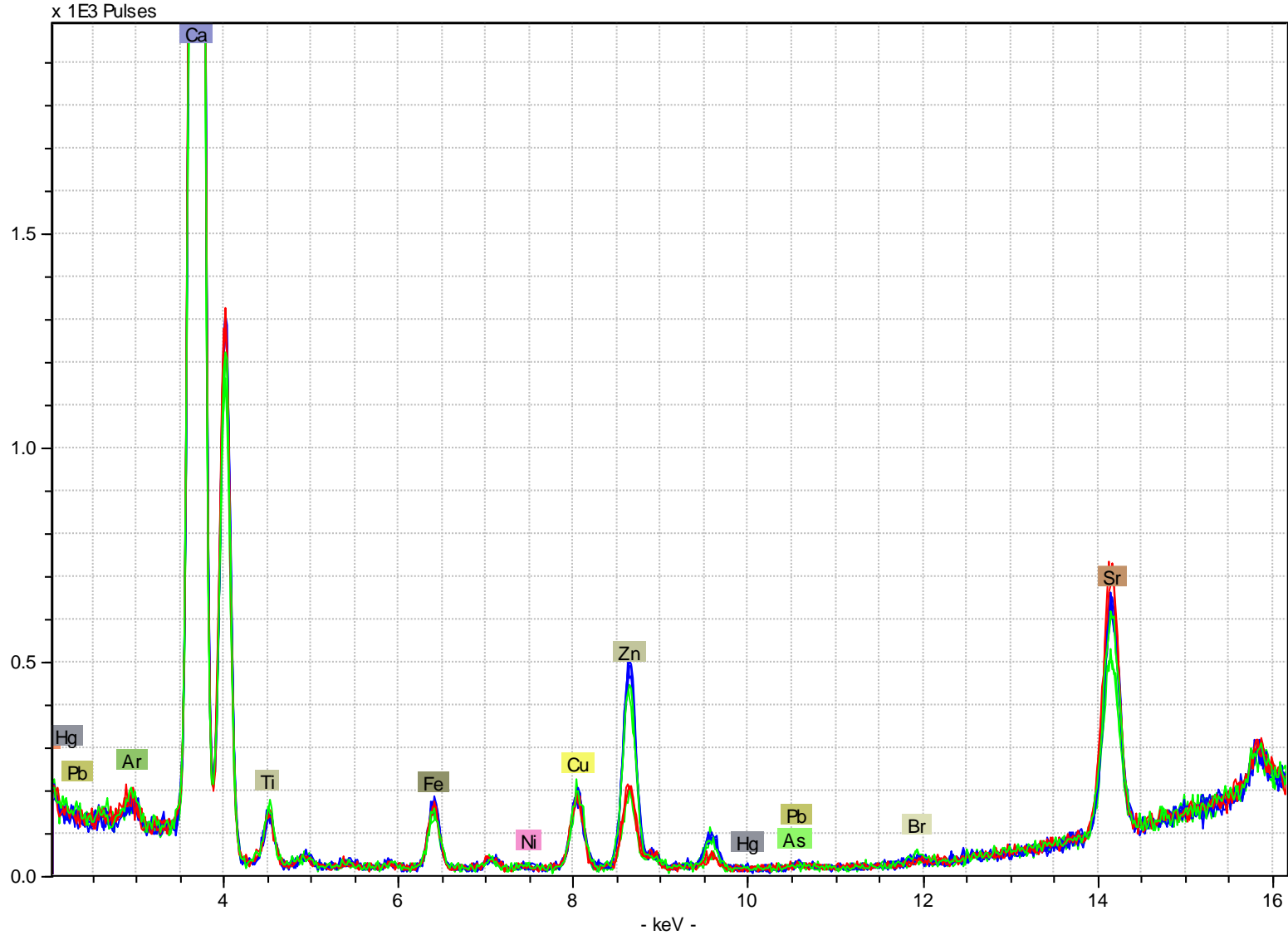


Figure 21: HHXRF spectra of M2, I1, and M3 from individual AH-K-29/6. Br stands for bromine; Sr stands for strontium. Ca stands for calcium. M2 is represented by green, I1 is represented by blue, and M3 is represented by red.

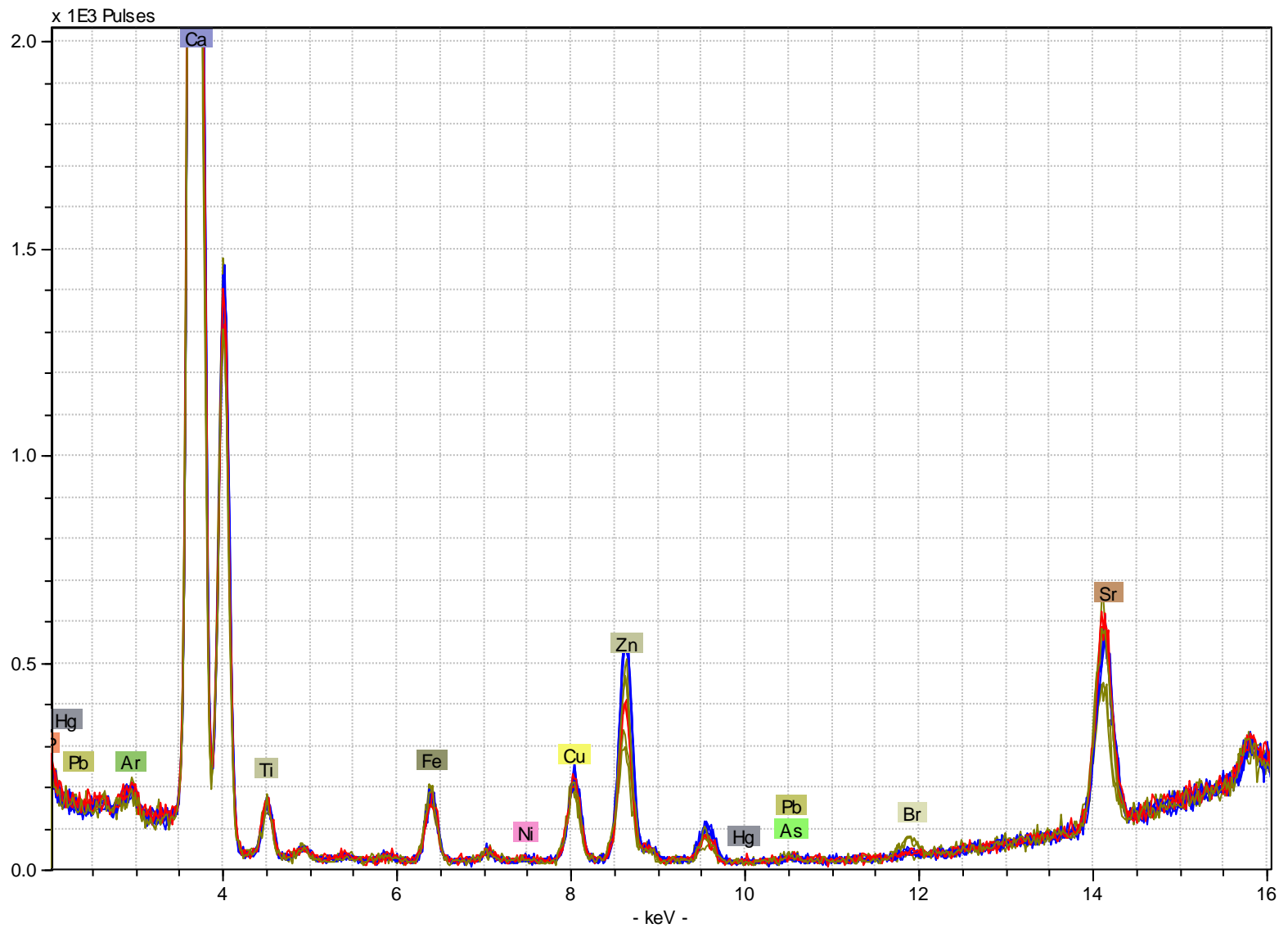


Figure 22: HHXRF spectra of M1, I1, and M3 from individual AH-K-29/8. Br stands for bromine; Sr stands for strontium. Ca stands for calcium. M1 is represented by gold, I1 is represented by blue, and M3 is represented by red.

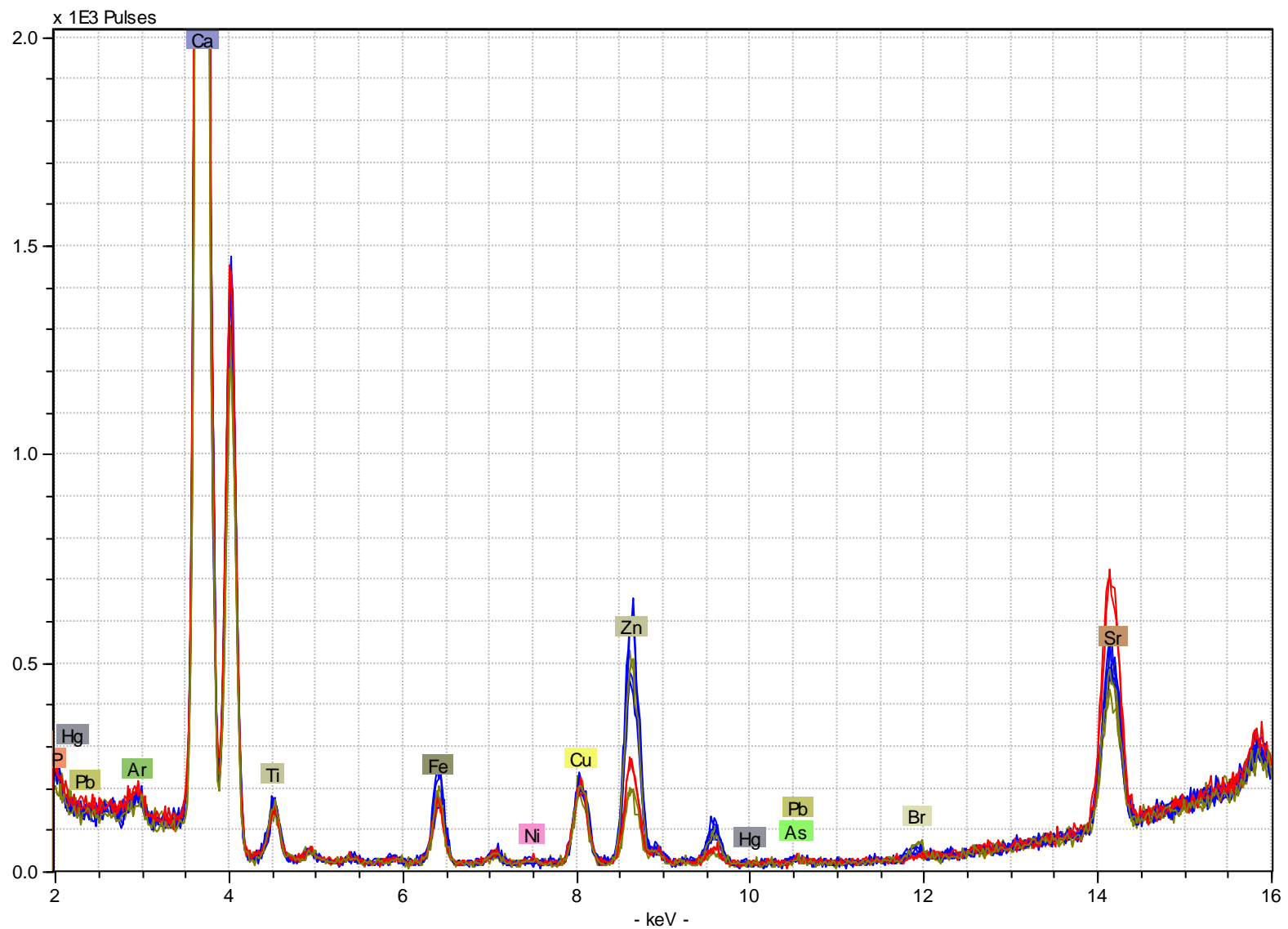


Figure 23: HHXRF spectra of M1, I1, and M3 from individual AH-K-29/18. Br stands for bromine; Sr stands for strontium. Ca stands for calcium. I1 is represented by blue, and M3 is represented by red.

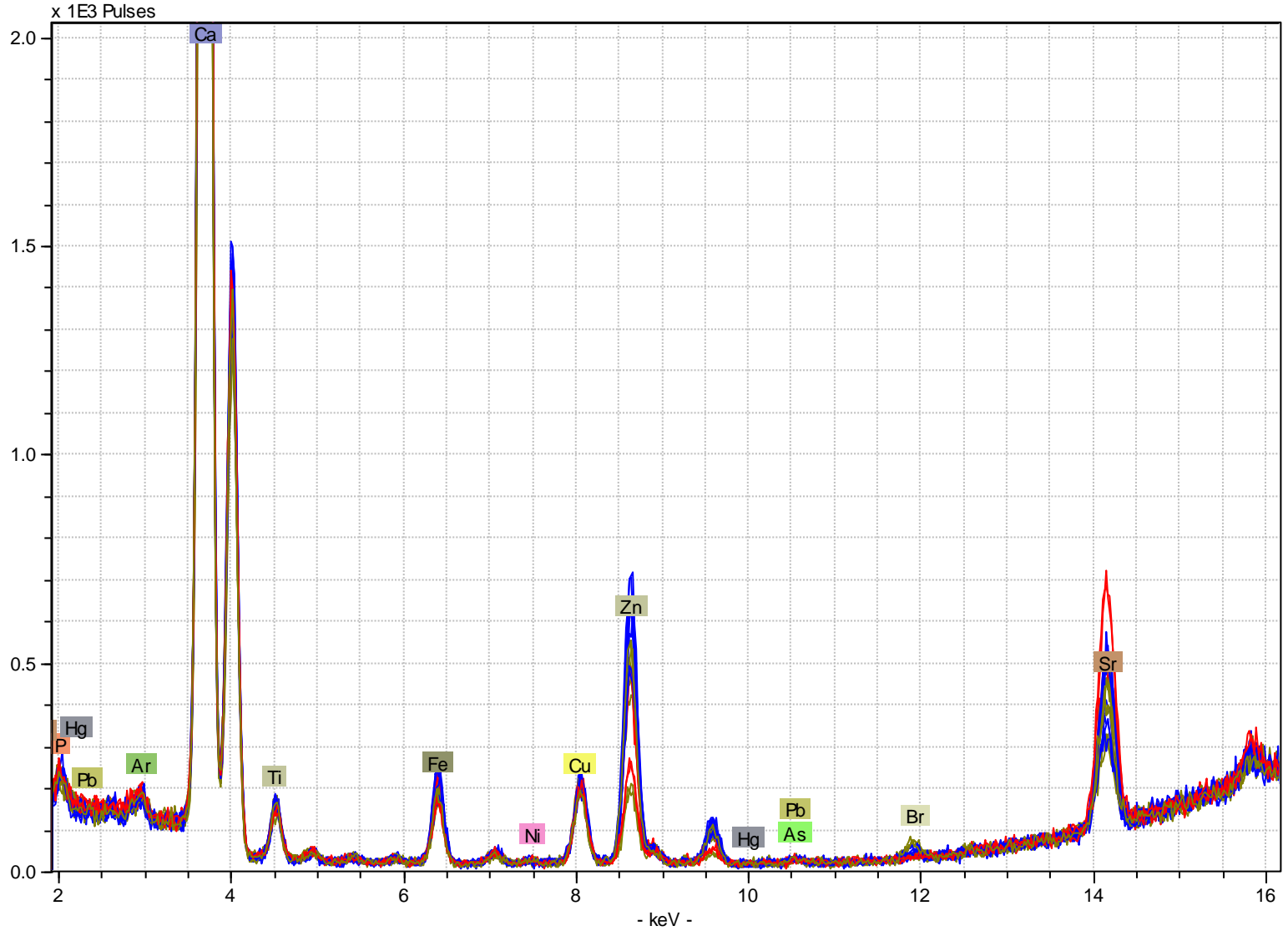


Figure 24: HHXRF spectra of M1, I1, and M3 from individual AH-K-29/19 Br stands for bromine; Sr stands for strontium. Ca stands for calcium. M1 is represented by gold, I1 is represented by blue, and M3 is represented by red.

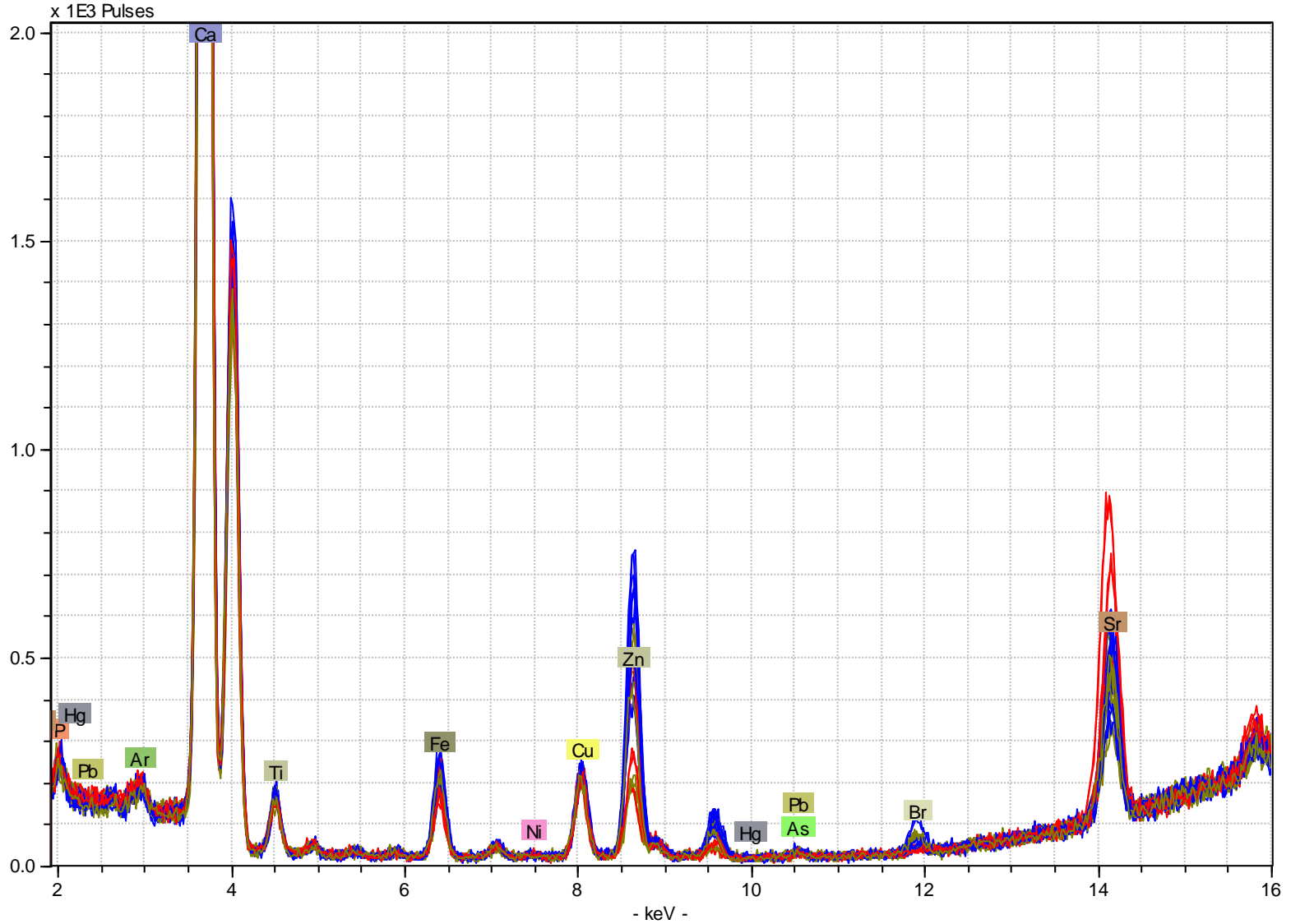


Figure 25: HHXRF spectra of M1, I1, and M3 from individual AH-K-35/5. Br stands for bromine; Sr stands for strontium. Ca stands for calcium. M1 is represented by gold, I1 is represented by blue, and M3 is represented by red.

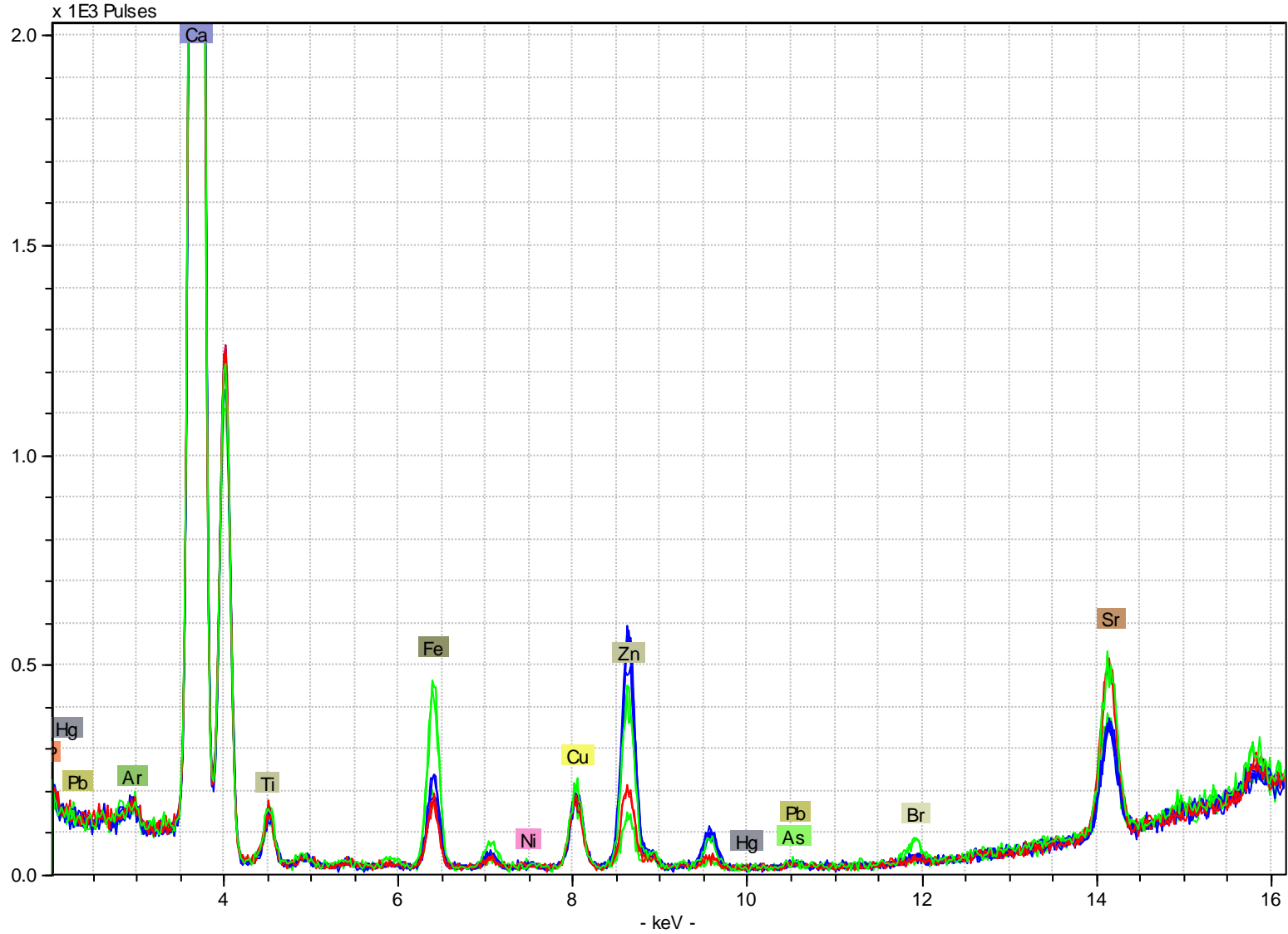


Figure 26: HHXRF spectra of M2, I1, and M3 from individual AH-K-35/6. Br stands for bromine; Sr stands for strontium. Ca stands for calcium. M2 is represented by green, I1 is represented by blue, and M3 is represented by red.

APPENDIX B: NET PHOTON COUNTS

Table 4: Net photon counts of each element per assay per sample.

INDIVIDUAL	TOOTH	SURFACE	BR K12	CA K12	P K12	SR K12
C-13-5-A	I1	L	147	52203	711	3436
C-13-5-A	I1	L	151	52176	545	3704
C-13-5-A	I1	P	9	52858	556	3252
C-13-5-A	I1	P	71	52979	535	3325
C-13-5-A	M1	C	658	55060	421	6011
C-13-5-A	M1	C	652	54543	690	6069
C-13-5-A	M1	M	356	52767	415	5376
C-13-5-A	M1	M	423	52767	510	5203
C-13-5-A	M3	C	17	51687	587	11222
C-13-5-A	M3	C	0	50255	511	11055
C-13-5-D	I1	L	94	51386	601	4479
C-13-5-D	I1	L	39	49777	446	4201
C-13-5-D	I1	P	119	51866	466	4227
C-13-5-D	I1	P	91	52085	691	4366
C-13-5-D	M1	C	1	47450	523	3434
C-13-5-D	M1	C	34	45267	644	3476
C-13-5-D	M1	M	221	41935	442	4476
C-13-5-D	M1	M	322	42028	509	4553
C-13-14	M3	C	122	58387	600	7866
C-13-14	M3	C	113	57554	561	7480
C-13-14	I1	L	48	58272	659	4933
C-13-14	I1	L	48	56288	630	5021
C-13-14	I1	P	230	54935	608	4573
C-13-14	I1	P	181	56894	830	4731
C-13-14	M2	C	139	56484	656	3986
C-13-14	M2	C	113	59411	686	4508
C-13-14	M2	M	966	57369	625	8472
C-13-14	M2	M	894	56329	489	7942
C-13-20	I1	L	202	54034	532	4230
C-13-20	I1	L	190	57531	697	4813
C-13-20	I1	P	239	55611	626	5108
C-13-20	I1	P	234	55761	606	5031
C-13-20	M2	C	188	51175	615	4339
C-13-20	M2	C	191	52253	482	4394
C-13-20	M2	M	584	48239	415	6933
C-13-20	M2	M	529	49725	430	7007
C-13-33	M3	C	254	62281	847	5399
C-13-33	M3	C	201	58628	686	5009

INDIVIDUAL	TOOTH	SURFACE	BR K12	CA K12	P K12	SR K12
C-13-33	I1	L	135	56881	642	5496
C-13-33	I1	P	1204	58616	711	8158
C-13-33	I1	P	208	55489	555	5417
C-13-33	M2	M	155	53099	550	3764
C-13-33	M2	M	181	58576	521	4220
C-13-33	M2	M	1276	54945	411	9001
C-13-33	M2	M	1293	58133	561	9405
E-44-2	M3	C	61	51769	507	6281
E-44-2	M3	C	8	50354	627	6257
E-44-2	I1	L	69	57698	665	6131
E-44-2	I1	L	37	53914	572	5947
E-44-2	I1	P	150	44200	526	4688
E-44-2	I1	P	87	42996	480	4336
E-44-2	M2	C	88	50808	519	5431
E-44-2	M2	C	416	53014	561	5898
E-44-2	M2	M	379	51717	492	5641
E-44-2	M2	M	494	54046	475	5858
E-44-3	I1	L	50	49804	630	10279
E-44-3	I1	L	1	50532	535	10369
E-44-3	I1	P	373	46278	507	10996
E-44-3	I1	P	403	49317	516	11646
E-44-3	M2	C	144	49802	592	10379
E-44-3	M2	C	211	48401	515	10151
E-44-3	M2	M	710	43912	525	9392
E-44-3	M2	M	762	47672	537	10064
E-44-7	M3	C	162	44656	387	3307
E-44-7	M3	C	117	44854	456	3450
E-44-7	I1	L	118	48265	565	3616
E-44-7	I1	L	120	47487	502	3611
E-44-7	I1	P	257	46358	433	3811
E-44-7	I1	P	273	44432	392	3825
E-44-7	M2	C	118	45842	484	3441
E-44-7	M2	C	113	42705	386	3105
E-44-7	M2	M	82	43934	644	3531
E-44-7	M2	M	120	44434	507	3602
E-44-8	I1	L	254	49480	573	3490
E-44-8	I1	L	265	50365	536	3237
E-44-8	I1	P	235	43179	564	3084
E-44-8	I1	P	208	45641	606	3492

INDIVIDUAL	TOOTH	SURFACE	BR K12	CA K12	P K12	SR K12
E-44-8	M2	C	121	47717	528	3194
E-44-8	M2	C	77	47301	409	3162
E-44-8	M2	M	312	50615	628	3773
E-44-8	M2	M	267	55204	681	3881
E-44-10	I1	L	377	54720	606	7866
E-44-10	I1	L	472	51376	467	7037
E-44-10	I1	P	251	53685	677	5018
E-44-10	I1	P	307	53777	733	5117
E-44-10	M2	C	223	53943	609	5203
E-44-10	M2	C	183	54244	657	5342
E-44-10	M2	M	819	57678	706	6002
E-44-10	M2	M	705	55361	731	5939
K-29-6	M3	C	67	55758	589	7668
K-29-6	M3	C	57	54184	577	7528
K-29-6	I1	L	165	56175	602	6722
K-29-6	I1	L	169	56014	605	6912
K-29-6	I1	P	142	55918	490	6973
K-29-6	I1	P	199	58450	576	7048
K-29-6	M2	C	50	49010	612	5094
K-29-6	M2	C	1	52326	552	5525
K-29-6	M2	M	224	51936	530	6583
K-29-6	M2	M	259	47992	511	5920
K-29-8	M3	C	60	54861	673	5843
K-29-8	M3	C	165	51865	635	5674
K-29-8	I1	L	85	54865	641	5155
K-29-8	I1	L	81	55101	760	5083
K-29-8	I1	P	56	56429	613	5505
K-29-8	I1	P	100	56571	696	5459
K-29-8	M1	C	26	56570	597	4026
K-29-8	M1	C	34	55915	670	3919
K-29-8	M1	M	422	54048	541	5709
K-29-8	M1	M	512	51303	545	5612
K-29-18	M3	C	17	54769	570	6914
K-29-18	M3	C	53	56170	595	7124
K-29-18	I1	L	243	55526	664	5139
K-29-18	I1	L	183	54153	596	4949
K-29-18	I1	P	132	55462	613	4420
K-29-18	I1	P	137	53977	657	4399
K-29-19	M3	C	1	53327	511	4483

INDIVIDUAL	TOOTH	SURFACE	BR K12	CA K12	P K12	SR K12
K-29-19	M3	C	42	53691	566	4537
K-29-19	I1	L	73	58826	696	3193
K-29-19	I1	L	78	53991	553	2849
K-29-19	I1	P	1	53530	475	2772
K-29-19	I1	P	22	50928	596	2678
K-29-19	M1	C	50	51262	472	2400
K-29-19	M1	C	27	51576	678	2318
K-29-19	M1	M	359	54651	575	3433
K-29-19	M1	M	326	53320	628	3438
K-35-5	M3	C	86	52807	601	8862
K-35-5	M3	C	98	51995	747	8962
K-35-5	I1	L	244	57579	490	4089
K-35-5	I1	L	207	57763	638	3805
K-35-5	I1	P	797	52006	492	5512
K-35-5	I1	P	796	51808	552	5357
K-35-5	M1	C	95	53556	720	3735
K-35-5	M1	C	63	53363	624	3605
K-35-5	M1	M	357	58276	691	4891
K-35-5	M1	M	423	52170	617	4152
K-35-6	M3	C	97	48648	580	4523
K-35-6	M3	C	48	48273	493	4671
K-35-6	I1	L	125	48033	468	3010
K-35-6	I1	L	160	49074	464	3304
K-35-6	I1	P	1	48109	463	2756
K-35-6	I1	P	143	49713	552	2986
K-35-6	M2	C	1	45759	352	3108
K-35-6	M2	C	52	45100	451	3080
K-35-6	M2	M	510	49123	418	4564
K-35-6	M2	M	573	48030	359	4564

M1, first molar; I1, first incisor; M2, second molar; M3; third molar; L, labial; P, palatal; C, crown, M, mesial; Br, bromine; Ca, calcium; P, phosphorous; Sr, strontium.

APPENDIX C: TRACE ELEMENT NET PHOTON COUNT RATIOS

Table 5: Net photon count ratios for each assay per sample. Bolded values were excluded from analysis.

INDIVIDUAL	TOOTH	SURFACE	SR/CA RATIO	BR/CA RATIO	CA/P RATIO
C-13-5-A	I1	L	0.06581997	0.00281593	73.4219409
C-13-5-A	I1	L	0.07099049	0.002894051	95.7357798
C-13-5-A	I1	P	0.06152333	0.000170268	95.0683453
C-13-5-A	I1	P	0.06276072	0.001340154	99.0261682
C-13-5-A	M1	C	0.10917181	0.011950599	130.783848
C-13-5-A	M1	C	0.11127001	0.011953871	79.0478261
C-13-5-A	M1	M	0.10188186	0.006746641	127.149398
C-13-5-A	M1	M	0.09860329	0.008016374	103.464706
C-13-5-A	M3	C	0.21711455	0.000328903	88.0528109
C-13-5-A	M3	C	0.21997811	0	98.3463796
C-13-5-D	I1	L	0.08716382	0.001829292	85.5008319
C-13-5-D	I1	L	0.08439641	0.000783494	111.607623
C-13-5-D	I1	P	0.08149848	0.002294374	111.300429
C-13-5-D	I1	P	0.08382452	0.001747144	75.3762663
C-13-5-D	M1	C	0.07237092	2.10748E-05	90.7265774
C-13-5-D	M1	C	0.07678883	0.000751099	70.2903727
C-13-5-D	M1	M	0.10673662	0.005270061	94.8755656
C-13-5-D	M1	M	0.10833254	0.007661559	82.5697446
C-13-14	M3	C	0.13472177	0.002089506	97.3116667
C-13-14	M3	C	0.1299649	0.001963374	102.5918
C-13-14	I1	L	0.08465472	0.000823723	88.4248862
C-13-14	I1	L	0.08920196	0.000852757	89.3460317
C-13-14	I1	P	0.08324383	0.004186766	90.3536184
C-13-14	I1	P	0.08315464	0.003181355	68.546988
C-13-14	M2	C	0.07056866	0.002460874	86.1036585
C-13-14	M2	C	0.0758782	0.001902005	86.6049563
C-13-14	M2	M	0.14767557	0.016838362	91.7904
C-13-14	M2	M	0.14099309	0.015871043	115.192229
C-13-20	I1	L	0.07828404	0.003738387	101.567669
C-13-20	I1	L	0.08365924	0.003302567	82.5408895
C-13-20	I1	P	0.09185233	0.004297711	88.8354633
C-13-20	I1	P	0.09022435	0.004196481	92.0148515
C-13-20	M2	C	0.08478749	0.003673669	83.2113821
C-13-20	M2	C	0.08409087	0.003655293	108.408714
C-13-20	M2	M	0.14372188	0.012106387	116.238554
C-13-20	M2	M	0.14091503	0.010638512	115.639535
C-13-33	M3	C	0.08668775	0.00407829	73.5312869

INDIVIDUAL	TOOTH	SURFACE	SR/CA RATIO	BR/CA RATIO	CA/P RATIO
C-13-33	M3	C	0.08543699	0.003428396	85.4635569
C-13-33	I1	L	0.09662277	0.002373376	88.5996885
C-13-33	I1	P	0.13917702	0.020540467	82.4416315
C-13-33	I1	P	0.09762295	0.003748491	99.9801802
C-13-33	M2	M	0.07088646	0.002919076	96.5436364
C-13-33	M2	M	0.07204316	0.003090003	112.429942
C-13-33	M2	M	0.16381836	0.023223223	133.686131
C-13-33	M2	M	0.16178418	0.0222421	103.623886
E-44-2	M3	C	0.12132744	0.001178311	102.108481
E-44-2	M3	C	0.12426024	0.000158875	80.3094099
E-44-2	I1	L	0.10626018	0.001195882	86.7639098
E-44-2	I1	L	0.1103053	0.000686278	94.2552448
E-44-2	I1	P	0.10606335	0.003393665	84.0304183
E-44-2	I1	P	0.10084659	0.002023444	89.575
E-44-2	M2	C	0.10689262	0.001732011	97.8959538
E-44-2	M2	C	0.11125363	0.007846984	94.4991087
E-44-2	M2	M	0.10907439	0.007328345	105.115854
E-44-2	M2	M	0.10838915	0.009140362	113.781053
E-44-3	I1	L	0.20638905	0.001003935	79.0539683
E-44-3	I1	L	0.20519671	1.97894E-05	94.4523364
E-44-3	I1	P	0.2376075	0.008059985	91.2781065
E-44-3	I1	P	0.23614575	0.008171624	95.5755814
E-44-3	M2	C	0.20840528	0.00289145	84.125
E-44-3	M2	C	0.20972707	0.004359414	93.9825243
E-44-3	M2	M	0.21388231	0.016168701	83.6419048
E-44-3	M2	M	0.21110925	0.015984226	88.7746741
E-44-7	M3	C	0.074055	0.003627732	115.390181
E-44-7	M3	C	0.07691622	0.002608463	98.3640351
E-44-7	I1	L	0.07491971	0.002444836	85.4247788
E-44-7	I1	L	0.07604186	0.002527007	94.5956175
E-44-7	I1	P	0.08220803	0.005543811	107.062356
E-44-7	I1	P	0.0860866	0.00614422	113.346939
E-44-7	M2	C	0.07506217	0.002574059	94.714876
E-44-7	M2	C	0.07270811	0.00264606	110.634715
E-44-7	M2	M	0.08037056	0.001866436	68.2204969
E-44-7	M2	M	0.08106405	0.002700635	87.6410256
E-44-8	I1	L	0.07053355	0.005133387	86.3525305
E-44-8	I1	L	0.06427082	0.00526159	93.9645522
E-44-8	I1	P	0.07142361	0.00544246	76.5585106

INDIVIDUAL	TOOTH	SURFACE	SR/CA RATIO	BR/CA RATIO	CA/P RATIO
E-44-8	I1	P	0.07651016	0.004557306	75.3151815
E-44-8	M2	C	0.06693631	0.002535784	90.3731061
E-44-8	M2	C	0.06684848	0.001627873	115.650367
E-44-8	M2	M	0.07454312	0.006164181	80.5971338
E-44-8	M2	M	0.07030288	0.004836606	81.0631424
E-44-10	I1	L	0.14375	0.00688962	90.2970297
E-44-10	I1	L	0.13697057	0.009187169	110.012848
E-44-10	I1	P	0.09347117	0.004675421	79.2983752
E-44-10	I1	P	0.0951522	0.00570876	73.3656207
E-44-10	M2	C	0.09645366	0.004133993	88.5763547
E-44-10	M2	C	0.09848094	0.003373645	82.5631659
E-44-10	M2	M	0.10406047	0.014199521	81.6968839
E-44-10	M2	M	0.10727769	0.012734597	75.7332421
K-29-6	M3	C	0.13752287	0.001201621	94.6655348
K-29-6	M3	C	0.138934	0.001051971	93.9064125
K-29-6	I1	L	0.11966177	0.00293725	93.3139535
K-29-6	I1	L	0.12339772	0.003017103	92.585124
K-29-6	I1	P	0.12470045	0.002539433	114.118367
K-29-6	I1	P	0.12058169	0.003404619	101.475694
K-29-6	M2	C	0.10393797	0.0010202	80.0816993
K-29-6	M2	C	0.10558804	1.9111E-05	94.7934783
K-29-6	M2	M	0.12675216	0.004313001	97.9924528
K-29-6	M2	M	0.12335389	0.005396733	93.9178082
K-29-8	M3	C	0.10650553	0.001093673	81.5170877
K-29-8	M3	C	0.1093994	0.003181336	81.6771654
K-29-8	I1	L	0.0939579	0.001549257	85.5928237
K-29-8	I1	L	0.09224878	0.001470028	72.5013158
K-29-8	I1	P	0.09755622	0.000992398	92.0538336
K-29-8	I1	P	0.09649821	0.00176769	81.2801724
K-29-8	M1	C	0.07116846	0.000459608	94.7571189
K-29-8	M1	C	0.07008853	0.000608066	83.4552239
K-29-8	M1	M	0.10562833	0.007807874	99.9038817
K-29-8	M1	M	0.10938931	0.009979923	94.133945
K-29-18	M3	C	0.1262393	0.000310395	96.0859649
K-29-18	M3	C	0.12682927	0.000943564	94.4033613
K-29-18	I1	L	0.09255124	0.004376328	83.623494
K-29-18	I1	L	0.09138921	0.003379314	90.8607383
K-29-18	I1	P	0.07969421	0.002380008	90.4763458
K-29-18	I1	P	0.08149767	0.002538118	82.1567732

INDIVIDUAL	TOOTH	SURFACE	SR/CA RATIO	BR/CA RATIO	CA/P RATIO
K-29-19	M3	C	0.08406623	1.87522E-05	104.358121
K-29-19	M3	C	0.08450206	0.000782254	94.860424
K-29-19	I1	L	0.05427872	0.001240948	84.5201149
K-29-19	I1	L	0.05276805	0.001444685	97.6329114
K-29-19	I1	P	0.05178405	1.86811E-05	112.694737
K-29-19	I1	P	0.05258404	0.000431982	85.4496644
K-29-19	M1	C	0.04681831	0.000975381	108.605932
K-29-19	M1	C	0.04494338	0.000523499	76.0707965
K-29-19	M1	M	0.06281678	0.006568956	95.0452174
K-29-19	M1	M	0.06447862	0.006114029	84.9044586
K-35-5	M3	C	0.16781866	0.001628572	87.8652246
K-35-5	M3	C	0.17236273	0.001884797	69.605087
K-35-5	I1	L	0.07101547	0.004237656	117.508163
K-35-5	I1	L	0.06587262	0.003583609	90.5376176
K-35-5	I1	P	0.10598777	0.015325155	105.703252
K-35-5	I1	P	0.10340102	0.015364422	93.8550725
K-35-5	M1	C	0.06974009	0.001773844	74.3833333
K-35-5	M1	C	0.06755617	0.001180593	85.5176282
K-35-5	M1	M	0.0839282	0.006126021	84.3357453
K-35-5	M1	M	0.07958597	0.008108108	84.554295
K-35-6	M3	C	0.09297402	0.001993915	83.8758621
K-35-6	M3	C	0.09676217	0.000994345	97.9168357
K-35-6	I1	L	0.06266525	0.002602378	102.634615
K-35-6	I1	L	0.06732689	0.003260382	105.762931
K-35-6	I1	P	0.05728658	2.07861E-05	103.907127
K-35-6	I1	P	0.06006477	0.002876511	90.0597826
K-35-6	M1	C	0.06792106	2.18536E-05	129.997159
K-35-6	M1	C	0.06829268	0.001152993	100
K-35-6	M1	M	0.09290963	0.010382102	117.519139
K-35-6	M1	M	0.09502394	0.011930044	133.788301

M1, first molar; I1, first incisor; M2, second molar; M3; third molar; L, labial; P, palatal; C, crown, M, mesial; Br, bromine; Ca, calcium; P, phosphorous; Sr, strontium.

APPENDIX D: TRACE ELEMENT NET PHOTON COUNT RATIO MEANS

Table 6: Net photon count ratio means per individual per tooth.

INDIVIDUAL	TOOTH	SR/CA RATIO MEAN	BR/CA RATIO MEAN
AH-C-13-14	M1	NA	NA
AH-C-13-14	I1	0.08506379	0.00226115
AH-C-13-14	M2	0.1087789	0.00926807
AH-C-13-14	M3	0.1323433	0.00202644
AH-C-13-20	M1	NA	NA
AH-C-13-20	I1	0.08600499	0.00388379
AH-C-13-20	M2	0.1133788	0.00751847
AH-C-13-20	M3	NA	NA
AH-C-13-33	M1	NA	NA
AH-C-13-33	I1	0.1111409	0.00888744
AH-C-13-33	M2	0.117133	0.0128686
AH-C-13-33	M3	0.08606237	0.00375334
AH-C-13-5-A	M1	0.1052317	0.00966687
AH-C-13-5-A	I1	0.06527363	0.0018051
AH-C-13-5-A	M2	NA	NA
AH-C-13-5-A	M3	0.2185463	0.0003289
AH-C-13-5-D	M1	0.09105723	0.00456091
AH-C-13-5-D	I1	0.08422081	0.00166358
AH-C-13-5-D	M2	NA	NA
AH-C-13-5-D	M3	NA	NA
AH-E-44-10	M1	NA	NA
AH-E-44-10	I1	0.117336	0.00661524
AH-E-44-10	M2	0.1015682	0.00861044
AH-E-44-10	M3	NA	NA
AH-E-44-2	M1	NA	NA
AH-E-44-2	I1	0.1058689	0.00182482
AH-E-44-2	M2	0.1089024	0.00651193
AH-E-44-2	M3	0.1227938	0.00066859
AH-E-44-3	M1	NA	NA
AH-E-44-3	I1	0.2213348	0.00574518
AH-E-44-3	M2	0.210781	0.00985095
AH-E-44-3	M3	NA	NA
AH-E-44-7	M1	NA	NA
AH-E-44-7	I1	0.07981405	0.00416497
AH-E-44-7	M2	0.07730122	0.0024468
AH-E-44-7	M3	0.07548561	0.0031181
AH-E-44-8	M1	NA	NA
AH-E-44-8	I1	0.07068453	0.00509869

INDIVIDUAL	TOOTH	SR/CA RATIO MEAN	BR/CA RATIO MEAN
AH-E-44-8	M2	0.0696577	0.00379111
AH-E-44-8	M3	NA	NA
AH-K-29-18	M1	NA	NA
AH-K-29-18	I1	0.08628308	0.00316844
AH-K-29-18	M3	0.1265343	0.00062698
AH-K-29-19	M1	0.05476427	0.00354547
AH-K-29-19	I1	0.05285372	0.00103921
AH-K-29-19	M3	0.08428415	0.00078225
AH-K-29-6	I1	0.1220854	0.0029746
AH-K-29-6	M2	0.114908	0.00268248
AH-K-29-6	M3	0.1382284	0.0011268
AH-K-29-8	M1	0.08906866	0.00471387
AH-K-29-8	I1	0.09506528	0.00144484
AH-K-29-8	M3	0.1079525	0.00213751
AH-K-35-5	M1	0.07520261	0.00429714
AH-K-35-5	I1	0.08656922	0.00962771
AH-K-35-5	M3	0.1700907	0.00175668
AH-K-35-6	M1	0.08103683	0.00782171
AH-K-35-6	I1	0.06183587	0.00291309
AH-K-35-6	M3	0.09486809	0.00149413

M1, first molar; I1, first incisor; M2, second molar; M3; third molar; L, labial; P, palatal; C, crown, M, mesial; Br, bromine; Ca, calcium; P, phosphorous; Pb, lead; Sr, strontium.

REFERENCES

- Bergmann, Christine L.
2018 Elemental Analyses of Archaeological Bone Using PXRF, ICP-MS, and a Newly Developed Calibration to Assess Andean Paleodiets. USF Tampa Graduate Theses and Dissertations, Tampa, FL
- Bloch, Lindsay
2015 Use of Handheld XRF Bruker Tracer III-SD. Research Laboratories of Archaeology, The University of North Carolina at Chapel Hill
- Byrnes, Jennifer F., and Peter J. Bush
2016 Practical considerations in trace element analysis of bone by portable X-ray fluorescence. *Journal of Forensic Sciences* 61(4):1041–1045. DOI:10.1111/1556-4029.13103.
- Dolphin, Alexis E., Steven J. Naftel, Andrew J. Nelson, Ronald R. Martin, and Christine D. White
2013 Bromine in teeth and bone as an indicator of marine diet. *Journal of Archaeological Science* 40(4):1778–1786. DOI:10.1016/j.jas.2012.11.020.
- Forshaw, R.
2014 Dental indicators of ancient dietary patterns: dental analysis in archaeology. *British Dental Journal* 216(9):529–535. DOI:10.1038/sj.bdj.2014.353.
- Knudson, Kelly J., Charles Stanish, Maria Cecilia Lozada Cerna, Kym F. Faull, and Henry Tantaleán
2016 Intra-individual variability and strontium isotope measurements: A methodological study using $^{87}\text{Sr}/^{86}\text{Sr}$ data from Pampa de los Gentiles, Chincha Valley, Peru. *Journal of Archaeological Science, Reports* 5:590–597. DOI:10.1016/j.jasrep.2016.01.016.
- Koutamanis, Dafne, Georgia L. Roberts, and Anthony Dosseto
2021 Inter- and intra-individual variability of calcium and strontium isotopes in modern Tasmanian wombats. *Palaeogeography, Palaeoclimatology, Palaeoecology* 574(110435):110435. DOI:10.1016/j.palaeo.2021.110435.
- Kozachuk, M. S., T. K. Sham, R. R. Martin, and A. J. Nelson
2020 Bromine, a possible marine diet indicator? A hypothesis revisited: Bromine, a possible marine diet indicator? A hypothesis revisited. *Archaeometry* 62(6):1267–1279. DOI:10.1111/arc.12590.

- Licata, Marta, Alessandro Bonsignore, Rosa Boano, Francesca Monza, Ezio Fulcheri, and Rosagemma Ciliberti
 2020 Study, conservation and exhibition of human remains: the need of a bioethical perspective. *Acta bio-medica : Atenei Parmensis* 91(4):e2020110.
 DOI:10.23750/abm.v91i4.9674.
- Mariel, Jairo, Francisco Javier Gutiérrez Cantú, Ricardo Oliva, Humberto Mariel Murga, Francisco Ojeda-Gutierrez, Raul Marquez Preciado, Wulfrano Sanchez Meraz, and Alma Lilián Guerrero-Barrera
 2014 Concentration and distribution of trace elements in dental enamel using the energy-dispersive X-ray spectroscopy technique. *European Scientific Journal* 10(18):295.
- Martin, Ronald R., Steven J. Naftel, Andrew J. Nelson, and William D. Sapp Iii
 2007 Comparison of the distributions of bromine, lead, and zinc in tooth and bone from an ancient Peruvian burial site by X-ray fluorescence. *Canadian Journal of Chemistry* 85(10):831–836. DOI:10.1139/v07-100.
- Pate, F. Donald
 1994 Bone chemistry and paleodiet. *Journal of Archaeological Method and Theory* 1(2):161–209. DOI:10.1007/bf02231415.
- Schwartz, Theresa C.
 2021 Determining Dietary Niche in Primates Using Portable X-Ray Fluorescence. University of Northern Colorado, Greeley, Colorado
- Shackley, M. Steven
 2011 An introduction to X-ray fluorescence (XRF) analysis in archaeology. In *X-Ray Fluorescence Spectrometry (XRF) in Geoarchaeology*, pp. 7–44. Springer New York, New York, NY.
- Shackley, M. Steven
 2012 Portable X-ray Fluorescence Spectrometry (pXRF): The Good, the Bad, and the Ugly. *Archaeology Southwest Magazine*, Tucson, AZ
- Simpson, Rachel, David M. L. Cooper, Treena Swanston, Ian Coulthard, and Tamara L. Varney
 2021 Historical overview and new directions in bioarchaeological trace element analysis: a review. *Archaeological and Anthropological Sciences* 13(1):24.
 DOI:10.1007/s12520-020-01262-4.
- Walton, April Alyce
 2021 Non-destructive Trace Element Analysis of Burials from Moho Cay, Belize. Louisiana State University and Agricultural and Mechanical College, Baton Rouge, LA

- White, Christine D., David M. Pendergast, Fred J. Longstaffe, and Kimberley R. Law
2001 Social complexity and food systems at Altun Ha, Belize: The isotopic evidence. *Latin American Antiquity* 12(4):371–393. DOI:10.2307/972085.
- White, Christine D., and Henry P. Schwarcz
1989 Ancient Maya diet: as inferred from isotopic and elemental analysis of human bone. *Journal of Archaeological Science* 16(5):451–474. DOI:10.1016/0305-4403(89)90068-x.
- White, Tim D., Michael T. Black, and Pieter Arend Folkens
2011 *Human Osteology*. 3rd ed. Academic Press, San Diego, CA.
- Wright, L. E., and H. P. Schwarcz
1998 Stable carbon and oxygen isotopes in human tooth enamel: Identifying breastfeeding and weaning in prehistory. *Am. J. Phys. Anthropol.* 106: 1–18. *American Journal of Physical Anthropology* 106(3):411–411. DOI:10.1002/(sici)1096-8644(199807)106:3<411::aid-ajpa16>3.0.co;2-3.
- Wright, Lori E., Juan Antonio Valdés, James H. Burton, T. Douglas Price, and Henry P. Schwarcz
2010 The children of Kaminaljuyu: Isotopic insight into diet and long distance interaction in Mesoamerica. *Journal of Anthropological Archaeology* 29(2):155–178. DOI:10.1016/j.jaa.2010.01.002.
- Wytenbach, A., S. Bajo, V. Furrer, M. Langenauer, and L. Tobler
1997 The accumulation of arsenic, bromine and iodine in needles of Norway Spruce (*Picea Abies* [L.] karst.) At sites with low pollution. *Water, Air, and Soil Pollution* 94(3–4):417–430. DOI:10.1007/bf02406073.
- Zimmerman, Heather A., Cayli J. Meizel-Lambert, John J. Schultz, and Michael E. Sigman
2015 Chemical differentiation of osseous, dental, and non-skeletal materials in forensic anthropology using elemental analysis. *Science & Justice: Journal of the Forensic Science Society* 55(2):131–138. DOI:10.1016/j.scijus.2014.11.003.